



HAL
open science

Palladium(ii) pincer complexes of a C , C , C -NHC, diphosponium bis(ylide) ligand

Rachid Taakili, Christine Lepetit, Carine Guyard-Duhayon, Dmitry A.
Valyaev, Noël Lugan, Yves Canac

► **To cite this version:**

Rachid Taakili, Christine Lepetit, Carine Guyard-Duhayon, Dmitry A. Valyaev, Noël Lugan, et al..
Palladium(ii) pincer complexes of a C , C , C -NHC, diphosponium bis(ylide) ligand. Dalton
Transactions, 2019, 48 (5), pp.1709-1721. 10.1039/c8dt04316g . hal-02140710

HAL Id: hal-02140710

<https://hal.science/hal-02140710v1>

Submitted on 6 Nov 2020

HAL is a multi-disciplinary open access archive for the deposit and dissemination of scientific research documents, whether they are published or not. The documents may come from teaching and research institutions in France or abroad, or from public or private research centers.

L'archive ouverte pluridisciplinaire **HAL**, est destinée au dépôt et à la diffusion de documents scientifiques de niveau recherche, publiés ou non, émanant des établissements d'enseignement et de recherche français ou étrangers, des laboratoires publics ou privés.

Palladium(II) Pincer Complexes of a *C,C,C*-NHC, Diphosphonium Bis(Ylide) Ligand

Rachid Taakili, Christine Lepetit, Carine Duhayon, Dmitry A. Valyaev, Noël Lugan,
Yves Canac*

LCC–CNRS, Université de Toulouse, CNRS, Toulouse, France

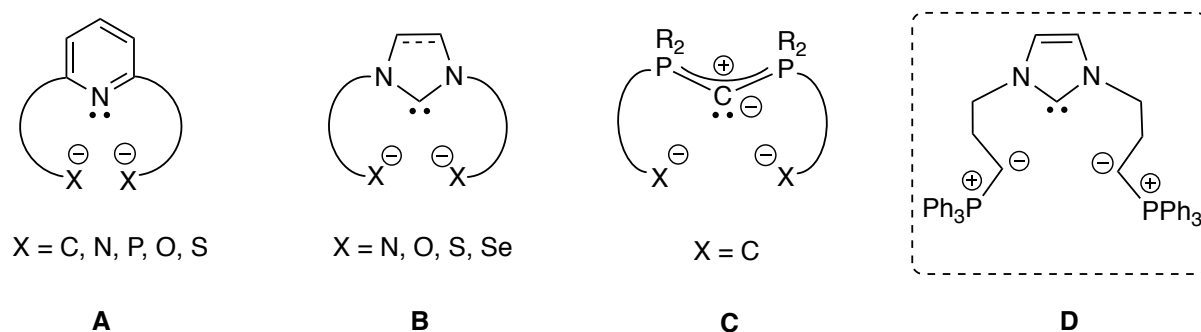
E-mail: yves.canac@lcc-toulouse.fr

Abstract: A new family of pincer palladium(II) complexes bearing an electron-rich *C,C,C*-NHC, diphosphonium bis(ylide) ligand of LX_2 -type was prepared through the dual N-functionalization of 1*H*-imidazole by (3-bromopropyl)triphenylphosphonium bromide. Selected basic conditions allowed the sequential coordination of the NHC and phosphonium ylide moieties to Pd(II). This strategy led to an original *ortho*-metallated complex where the Pd center is bonded to four carbon atoms of three different nature: carbenic (sp^2), arylic (sp^2), and chiral ylidic (sp^3). Protonation of the latter afforded NHC, diphosphonium bis(ylide) pincer Pd(II) complexes as the mixture of *meso*- and *dl*- diastereomers (de = 50%). The selectivity of C-coordination was rationalized on the basis of DFT calculations, evidencing the quasi-degeneracy of the two diastereomeric forms.

Keywords: Carbon ligand, NHC, palladium, phosphonium ylide, pincer complex.

Introduction

In the large family of polydentate ligands, pincer-type ligands are by far the most extensively investigated ones in recent years.¹ This huge craze is due to the propensity of such systems to adopt a robust meridional tridentate coordination mode, which leaves an open coordination shell forcing the adjacent coordination to any incoming molecule and preventing undesired ligand redistribution processes.² This peculiarity makes thus pincer ligands attractive auxiliaries for organometallic chemistry and homogeneous catalysis.³ The seminal pincer structure proposed by Shaw *et al.* was based on an anionic carbon center bearing two pendant phosphine donors.⁴ Since then, the structure of pincer ligands has been extremely diversified in order to finely tune their stereo-electronic properties and, as a consequence, the reactivity of the ensuing metal complexes. According to the Green formalism,⁵ neutral (L_3 -type), mono- (L_2X -type), di- (LX_2 -type), and tri-anionic (X_3 -type) pincer frameworks were designed allowing an efficient control of the metal coordination sphere and the stabilization of a broad range of metals with different oxidation states.⁶ While metal complexes supported by L_3 , and L_2X -type pincer ligands are the most common ones, those showing LX_2 -type ligands remain scarce. Considering only the cases where the central donor moiety is neutral, three substructures of the latter family can be mentioned, all having the intrinsic peculiarity of being dianionic in nature by their peripheral coordination moieties.⁷ Pyridine- (**A**),⁸ NHC- (**B**),⁹ and carbodiphosphorane (**C**)¹⁰ pincer architectures featuring two flanking donor arms with different coordinating atoms (C, N, P, O, S) were thus reported (Scheme 1). It should be noted that, to date, system **C** represents the only case of C,C,C -pincer ligand of LX_2 -type forming stable complexes.¹⁰

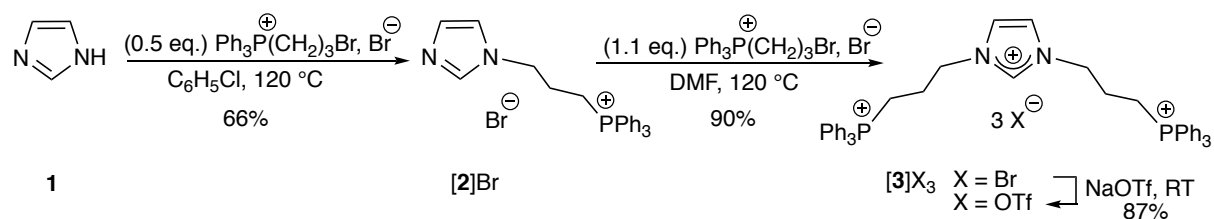


Scheme 1. Schematic representation of known LX_2 pincer-type ligands **A-C** and targeted NHC, diphosphonium bis(ylide) pincer ligand **D**.

Based on the recent preparation of metal complexes of electron-rich *C,C*-chelating NHC-phosphonium ylide ligands,¹¹ in the bi-¹² and in the tetradente series,¹³ we focused our interest on the design of pincer systems. The appropriate association of the two strongly σ -donor and relatively weakly π -acceptors carbon based ligands,¹⁴ both of which are charge-neutral in the free state (NHC: $N^+=C^-$, $2e^-$ donor (L type); ylide: P^+-C^- , $1e^-$ donor (X type)), should benefit the design of a new family of electron-rich LX_2 pincer-type ligand, which would differentiate from those already existing ones (A-C) by their global charge.¹⁵ The stereoselectivity of complexation of such hybrid chelating carbon based ligands might be influenced by conformational preferences due to the existence of non-covalent electrostatic interactions and/or hydrogen bonds as already observed in stabilized¹⁶ or more recently in non-stabilized bis-ylide derivatives.¹³ The present contribution addresses the preparation and the evaluation of the coordination properties towards palladium(II) centers of a new member of the restricted family of LX_2 pincer-type ligands, namely the *C,C,C*-NHC, diphosphonium bis(ylide) **D** (Scheme 1).¹⁷

Results and Discussion

The N-phosphonio-substituted imidazole [2]Br was prepared in 66% yield by treating 1*H*-imidazole **1** with 0.5 equivalent of (3-bromopropyl)triphenylphosphonium bromide in C_6H_5Cl at 120 °C (Scheme 2). The second phosphonium-bearing N-substituent was introduced by adding to the imidazole [2]Br an equivalent of the same phosphonium salt in DMF at 120 °C, allowing the bis(N-phosphonio)-imidazolium salt [3](Br)₃ to form, the latter being isolated in 90% yield.¹⁸ Because of the poor solubility of [3](Br)₃ in common solvents, an anion metathesis was conducted with NaOTf in CH_2Cl_2 leading to the corresponding more soluble salt [3](OTf)₃ in 87% yield (Scheme 2). As observed for the imidazole [2]Br (δ_P 23.9 ppm), the ³¹P NMR spectrum of imidazolium salts [3]X₃ displayed a single signal at δ_P 23.7 ppm (X = OTf) or δ_P 24.7 ppm (X = Br), in the typical range for phosphonium derivatives.¹⁹ The imidazolium protons of [3]X₃ were evidenced by the characteristic low field signal at δ_H 8.9 ppm (X = OTf) or δ_H 10.1 ppm (X = Br) in the ¹H NMR spectra. The structure of imidazolium [3](OTf)₃, as well as that of imidazole [2]Br, were unambiguously confirmed by single crystal X-ray diffraction analyses (Figure 1).²⁰



Scheme 2. Sequential preparation of N - $[(\text{CH}_2)_3\text{PPh}_3]^+$ substituted imidazolium salts $[\mathbf{3}]\text{X}_3$ ($\text{X} = \text{Br}, \text{OTf}$) from $1H$ -imidazole **1**.

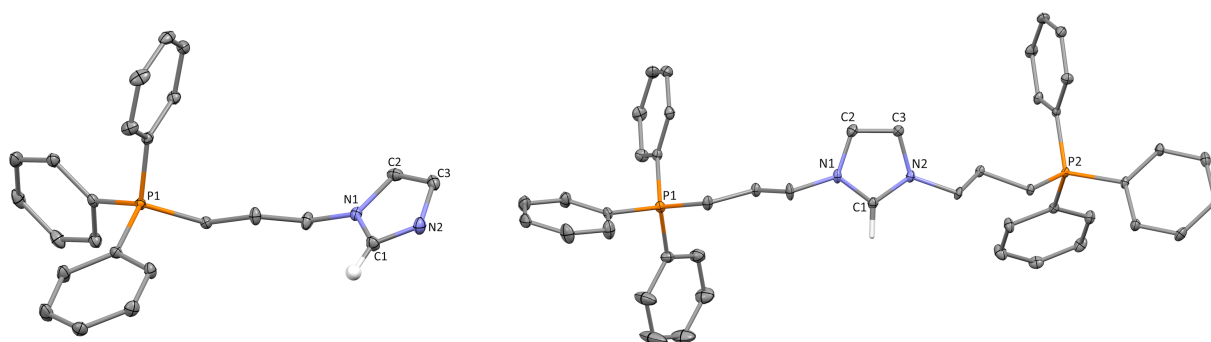
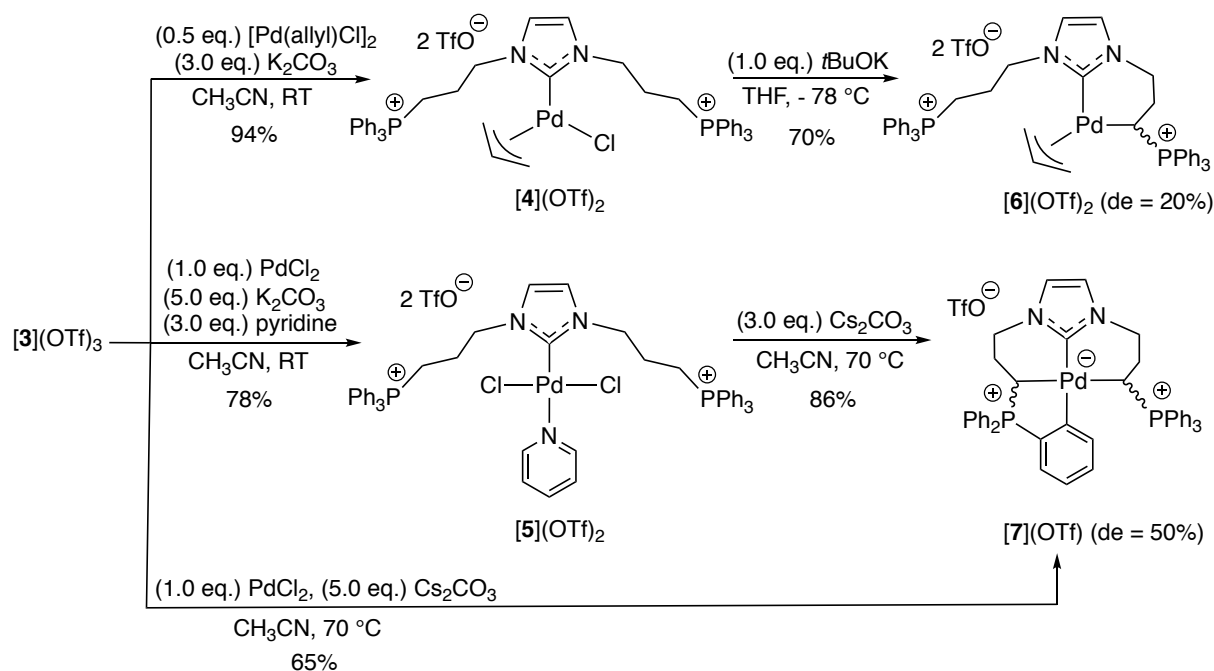


Figure 1. Perspective views of the cationic part of N -phosphonio-imidazole $[\mathbf{2}]\text{Br}$ (*left*), and bis(N -phosphonio)-imidazolium salt $[\mathbf{3}](\text{OTf})_3$ (*right*) with thermal ellipsoids drawn at the 30% probability level. The H atoms are omitted for clarity, except the one attached to the carbon atom C1. Selected bond lengths [\AA] and angles [$^\circ$]: $[\mathbf{2}]\text{Br}$: C1–N1 = 1.351(2); C1–N2 = 1.318(2); C2–C3 = 1.351(2); N1–C1–N2 = 112.09(15). $[\mathbf{3}](\text{OTf})_3$: C1–N1 = 1.328(5); C1–N2 = 1.330(4); C2–C3 = 1.352(6); N1–C1–N2 = 108.5(3).

The dual N -functionalization of imidazole **1** enabled the preparation of a new class of imidazolium salts bearing two phosphonium side chains, whose coordination properties were explored. On the basis of results obtained recently in the bi- and tetradentate series¹²⁻¹³ which showed a significant difference in the acidity of imidazolium and alkyl phosphonium H-atoms,²¹ a sequential strategy for the complexation of pre-ligand $[\mathbf{3}](\text{OTf})_3$ was envisioned. Treatment of $[\mathbf{3}](\text{OTf})_3$ with 0.5 equivalent of $[\text{PdCl}(\pi\text{-allyl})_2]$ in the presence of K_2CO_3 in CH_3CN cleanly afforded the bis(N -phosphonio)-(NHC) Pd(II) complex $[\mathbf{4}](\text{OTf})_2$ in 94% yield (Scheme 3, *up*). A similar coordination mode was observed upon addition of a stoichiometric amount of PdCl_2 to $[\mathbf{3}](\text{OTf})_3$ in the presence of the K_2CO_3 /pyridine system in CH_3CN , yielding the dicationic (NHC) PdCl_2 complex $[\mathbf{5}](\text{OTf})_2$ in 78% yield (Scheme 3, *bottom*).²² The formation of the NHC complexes $[\mathbf{4}](\text{OTf})_2$ and $[\mathbf{5}](\text{OTf})_2$ was clearly

indicated by ^1H NMR spectroscopy evidencing the disappearance of the characteristic ^1H imidazolium signal of the precursor $[\mathbf{3}](\text{OTf})_3$. In the complex $[\mathbf{5}](\text{OTf})_2$, the coordination of pyridine to the Pd center was confirmed by the presence of three ^1H NMR resonances at δ_{H} 7.48, 7.97, 8.71 ppm in the H_{ar} atom region. The unchanged environment of the phosphonium moieties within the Pd complexes $[\mathbf{4}](\text{OTf})_2$ and $[\mathbf{5}](\text{OTf})_2$ as compared to $[\mathbf{3}](\text{OTf})_3$ was illustrated by the similarity of their ^{31}P NMR chemical shifts ($[\mathbf{3}](\text{OTf})_3$: δ_{P} 23.7 ppm; $[\mathbf{4}](\text{OTf})_2$: δ_{P} 23.8 ppm; $[\mathbf{5}](\text{OTf})_2$: δ_{P} 23.7 ppm). In the ^{13}C NMR spectra, the N_2C -Pd carbon atoms of NHC complexes $[\mathbf{4}](\text{OTf})_2$ (δ_{C} 180.9 ppm) and $[\mathbf{5}](\text{OTf})_2$ (δ_{C} 150.7 ppm) were found to be deshielded with respect to the N_2CH carbon atom of precursor $[\mathbf{3}](\text{OTf})_3$ (δ_{C} 137.4 ppm). The dicationic character of Pd complexes $[\mathbf{4}](\text{OTf})_2$ and $[\mathbf{5}](\text{OTf})_2$ was also revealed by ESI mass spectroscopy ($\mathbf{4}^+$: m/z 1119.1 $[\text{M}-\text{Cl}]^+$; $\mathbf{5}^+$: m/z 1078.1 $[\text{M}-\text{TfO}]^+$) with the evidence of two non-coordinating TfO^- anions.



Scheme 3. Synthesis of the bis(N-phosfonio)-(NHC) Pd(II) complexes $[\mathbf{4}](\text{OTf})_2$ and $[\mathbf{5}](\text{OTf})_2$, and related NHC-phosponium ylide Pd(II) complexes $[\mathbf{6}](\text{OTf})_2$ and $[\mathbf{7}](\text{OTf})$ from the imidazolium salt $[\mathbf{3}](\text{OTf})_3$.

The exact structure of (NHC) Pd(II) complexes $[\mathbf{4}](\text{OTf})_2$ and $[\mathbf{5}](\text{OTf})_2$ were firmly established by X-ray diffraction analysis of single yellow crystals (Figure 2).²⁰ In both cases, the Pd atom resides in a quasi-square-planar environment where the coordinated plane defined by the C1, C67, C69, C11 atoms, and C1, C11, C11ⁱ, N3 atoms, respectively, are positioned

nearly orthogonally to the NHC ring ([**4**](OTf)₂: dihedral angle {N1–C1–Pd1–Cl1} = 88.67°; [**5**](OTf)₂: dihedral angle {N1–C1–Pd1–Cl1} = 86.65°). The N₂C–Pd bond distances ([**4**](OTf)₂: C1–Pd1 = 2.018(2) Å; [**5**](OTf)₂: C1–Pd1 = 1.956(3) Å) are in the typical range of related cationic (NHC) Pd(II) complexes.¹² In complex [**5**](OTf)₂, the pyridine ligand is located in *trans* position relative to the NHC core as generally observed in such complexes.²² A difference to be noted between the two Pd complexes concerns the position of the phosphonium chains relative to the carbenic ring. Indeed, while the two chains are located on the same side in [**4**](OTf)₂, they are on either side of the NHC moiety in complex [**5**](OTf)₂. Such a specific arrangement can be tentatively attributed to the presence of stabilizing electrostatic interactions between the phosphonium groups and the halogen atoms on the metal.

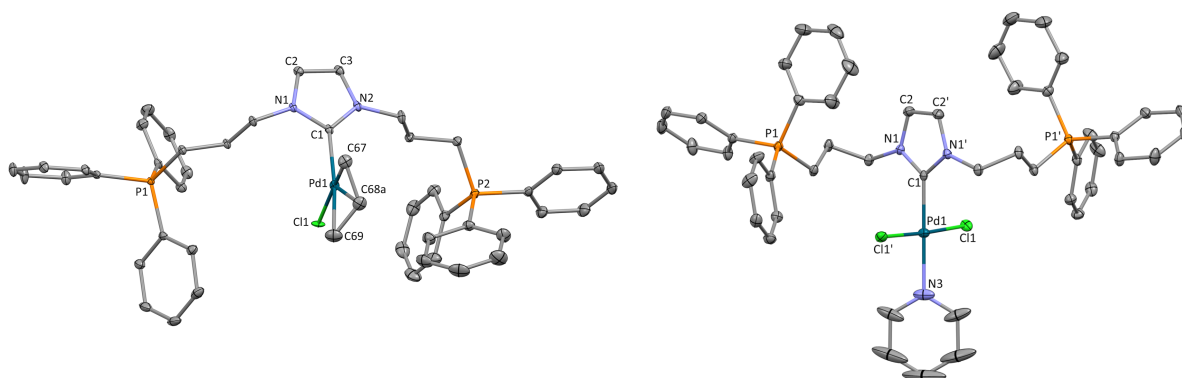


Figure 2. Perspective views of the cationic part of bis(N-phosponio)-substituted (NHC) Pd(II) complexes [**4**](OTf)₂ (*left*), and [**5**](OTf)₂ (*right*) with thermal ellipsoids drawn at the 30% probability level. The H atoms are omitted for clarity. Selected bond lengths [Å] and angles [°]: [**4**](OTf)₂: C1–N1 = 1.355(2); C1–N2 = 1.355(3); C2–C3 = 1.347(3); C1–Pd1 = 2.018(2); Pd1–Cl1 = 2.4039(6); Pd1–C67 = 2.094(3); Pd1–C69 = 2.209(4); N1–C1–N2 = 104.1(2); N1–C1–Pd1 = 124.6(2); C1–Pd1–Cl1 = 92.57(6); C1–Pd1–C67 = 97.0(1). [**5**](OTf)₂: C1–N1 = 1.345(3); C2–C2ⁱ = 1.345(4); C1–Pd1 = 1.956(3); Pd1–Cl1 = 2.3089(6); Pd1–N3 = 2.102(3); N1–C1–N1ⁱ = 105.6(2); N1–C1–Pd1 = 127.22(12); C1–Pd1–N3 = 180.00(1); C1–Pd1–Cl1 = 88.44(2); symmetry code: (i) 1–x, y, 3/2–z.

Anticipating the use of a sequential strategy for anchoring the ylide arms in direction on hitherto unknown NHC-phosphonium ylide pincer-type complexes, the NHC π -allyl Pd complex [**4**](OTf)₂ was treated with an equivalent of potassium *tert*-butoxyde (*t*BuOK) in THF at –78 °C. Under these conditions, the *C,C*-chelating NHC-phosphonium ylide π -allyl Pd(II) complex [**6**](OTf)₂ was isolated in 70% yield as a 60/40 mixture of two diastereoisomers (Scheme 3, *up*). The structure of Pd complex [**6**](OTf)₂ was first assigned on

the basis of the ^{31}P NMR spectrum, which exhibited two sets of resonances. Indeed, the pendant cationic chain displayed a set of singlets in the phosphonium region (major: δ_{P} 23.7 ppm; minor: δ_{P} 23.8 ppm), while the coordinated ylide was characterized by a set of singlets at a slightly lower field (major: δ_{P} 31.4 ppm; minor: δ_{P} 32.2 ppm). The linkage of the CH ylide moiety was also apparent from the upfield shift of the corresponding $^{13}\text{C}\{^1\text{H}\}$ NMR resonances (minor: δ_{CH} 2.0 ppm (d, $^1J_{\text{CP}} = 33.2$ Hz); major: δ_{CH} 2.1 ppm (d, $^1J_{\text{CP}} = 34.2$ Hz)). As commonly observed in related Pd(II) complexes, the occurrence of two diastereomers in solution for complex [6](OTf)₂ is due to the presence of the stereogenic ylidic carbon atom associated to the slow rotary flip of the π -allyl ligand.^{12,23}

The NHC-phosphonium ylide π -allyl Pd complex [6](OTf)₂ was treated next with an additional equivalent of base (*t*-BuOK) in order to induce the coordination of the pending cationic chain. However, no reaction was observed, even after addition of an excess of base. It is likely that the strongly chelating π -allyl ligand actually prevents the anchorage of the second ylidic carbon atom. To facilitate the chelation of the metal center by the two ylide extremities, the deprotonation of the analogous (NHC) PdCl₂ complex [5](OTf)₂ was considered as an alternative approach.

Disappointingly, whatever the conditions of the reaction (solvent, temperature, nature of the base), addition of two equivalents of base to [5](OTf)₂ did not lead to a selective reaction, several Pd–ylide species being indeed formed as evidenced by their characteristic ^{31}P NMR resonances.²⁴ This result confirmed the great acidity of the sp^3 CH₂ groups at the phosphonium fragments, but indicated also that other sites are reactive towards a base. The selectivity issue was finally circumvented by using an excess of base, more precisely by treating the PdCl₂ complex [5](OTf)₂ with 3 equiv of Cs₂CO₃ in CH₃CN at 70 °C. Under such conditions, the Pd complex [7](OTf) was formed selectively and isolated in 86% yield as a 75/25 mixture of two diastereomers. Although with a lesser yield of 65%, complex [7](OTf) could be also prepared through a one step procedure, by treating the imidazolium salt [3](OTf)₃ with PdCl₂ in the presence of an excess of Cs₂CO₃ in CH₃CN at 70 °C.

The occurrence of two diastereomers for Pd complex [7](OTf) was indicated by the presence of two sets of ^{31}P NMR resonances (major: δ_{P} 28.2 ppm (brs), 29.2 ppm (brs); minor: δ_{P} 23.3 ppm (s), 31.1 ppm (s)). For each isomer, detailed analysis of the ^1H NMR spectra revealed the absence of an H_{ar} atom belonging to one of the phosphonium moieties, thus suggesting a Csp^2 –H bond activation.²⁵ For instance for the major isomer, four distinct ^1H NMR resonances at δ_{H} 6.84, 7.00, 7.30, 8.27 ppm could be clearly assigned to the *o*-C₆H₄PPh₂Pd moiety. The same conclusion could be drawn from the ^{13}C NMR spectrum with the presence of the characteristic strongly deshielded signal of the *ortho*-metallated carbon

atom at δ_{C} 183.5 ppm (d, $^2J_{\text{CP}} = 36.2$ Hz), and the corresponding *ipso* quaternary carbon atom at δ_{C} 138.9 ppm (d, $^1J_{\text{CP}} = 116.7$ Hz). ^{13}C NMR spectroscopy also unveiled two different CH ylidic resonances at δ_{CH} 10.5 ppm (dd, $J_{\text{CP}} = 3.0, 21.1$ Hz); δ_{CH} 17.6 ppm (d, $^1J_{\text{CP}} = 37.2$ Hz)). Similar assignments could be done for the minor isomer of complex [7](OTf) (see experimental section). Noteworthy, the ^{13}C NMR signal of the carbenic carbon atoms of [7](OTf) underwent a significant shift upon coordination of the ylidic arms (major: δ_{C} 175.5 ppm, minor: δ_{C} 178.8 ppm; [5](OTf)₂: δ_{C} 150.7 ppm). The palladate negative charge was deduced from ESI mass spectroscopy (7^+ : m/z 777.2 [M-TfO]⁺) with the evidence of only one residual TfO⁻ anion.²⁶ In summary, the formation of Pd complex [7](OTf) showing C-coordination of the two ylides and the *ortho* C–H bond activation of a P⁺-phenyl substituent can be attributed to the excess of base used.

The Pd(II) complex [7](OTf) can be formally considered as a ‘constrained analogue’ of the expected NHC, bis(ylide) pincer complex where the reactive coordination site *trans* to the central NHC is somewhat ‘neutralized’ by the *ortho*-metallation of one of the P⁺-phenyl rings. We thus reasoned that the selective cleavage of the resulting C_{ar}–Pd bond could constitute an entry to the targeted LX₂ pincer-type complex. Gratifyingly, the addition of a stoichiometric amount of trifluoromethanesulfonic acid to [7](OTf) in CH₃CN at –40 °C cleanly afforded the desired NHC, bis(ylide) Pd(II) pincer complex [8](OTf)₂ (Scheme 4, *left*). The latter isolated in 94% yield as a 75/25 mixture of two diastereomers appeared to be perfectly stable in air both in the solid state and in solution, and could be easily prepared on a gram scale. The selective cleavage of the C_{ar}–Pd bond was indicated by the appearance of one singlet for each diastereomer in the ^{31}P NMR spectrum of complex [8](OTf)₂, in agreement with an expected C₂ or C_∞ symmetry. The chemical shifts of the ^{31}P NMR signals appearing at relatively high field (minor: δ_{P} 32.7, major: δ_{P} 33.8 ppm) confirmed that the stereogenic ylidic carbon atoms remained coordinated to the Pd center. The persistence of the Pd–CH bond was also corroborated by ^{13}C NMR spectroscopy, showing two sets of signals in the high-field region with proper multiplicity (major: δ_{CH} 7.8 ppm, (d, $^1J_{\text{CP}} = 30.9$ Hz); minor: δ_{CH} 9.9 ppm, (d, $^1J_{\text{CP}} = 32.8$ Hz)). The ^{13}C NMR signals of the N₂C center of [8](OTf)₂ (major: δ_{C} 160.1; minor: δ_{C} 161.4 ppm) was found in the typical range of carbenic carbon atoms. When recorded in CD₂Cl₂, the ^{13}C NMR spectrum showed the presence of a coordinated CH₃CN molecule as indicated by the corresponding single resonances (major: δ_{C} 1.6 ppm; minor: δ_{C} 2.3 ppm).²⁷ Noteworthy, protonation of the orthopalladated phenyl moiety did not alter the ratio of diastereomers (*ca.* 75/25) observed during the formation of Pd complex [7](OTf).

After many attempts, single crystals of complex [8](OTf)₂ suitable for an X-ray diffraction analysis were finally obtained in a CH₂Cl₂/Et₂O mixture at room temperature. Although the

poor quality of the single crystals did not permit at the end to discuss in detail the geometric parameters, the XRD analysis gave evidence of the targeted LX₂ pincer-type structure of the complex with its central NHC core and two phosphonium ylide arms occupying mutually *trans* positions (C6–Pd1–C9 = 173.2(4)°) (Figure 3). The coordination of the two ylides results in the formation of two fused six-membered palladacycles, an environment in which the Pd(II) atom adopts a distorted square planar geometry. The crystal structure could also confirm the presence of a coordinated molecule of acetonitrile in *trans* position to the NHC core. The sterically hindered PPh₃⁺ substituents attached to the stereogenic *sp*³ ylidic C6 and C9 carbon atoms are located on either side of the C₃NPd coordination plane conferring a *R*_{C6},*R*_{C9} (*S*_{C6},*S*_{C9}) configuration to the crystallized diastereomer (*dl* form).

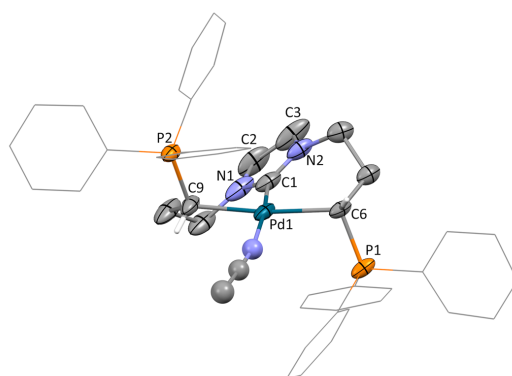
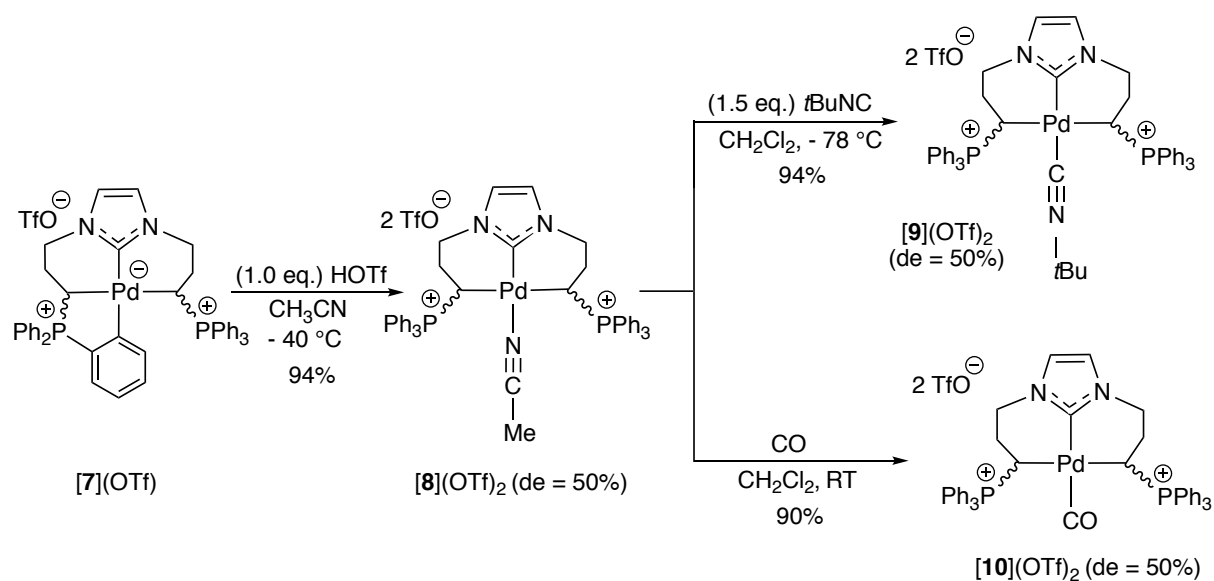
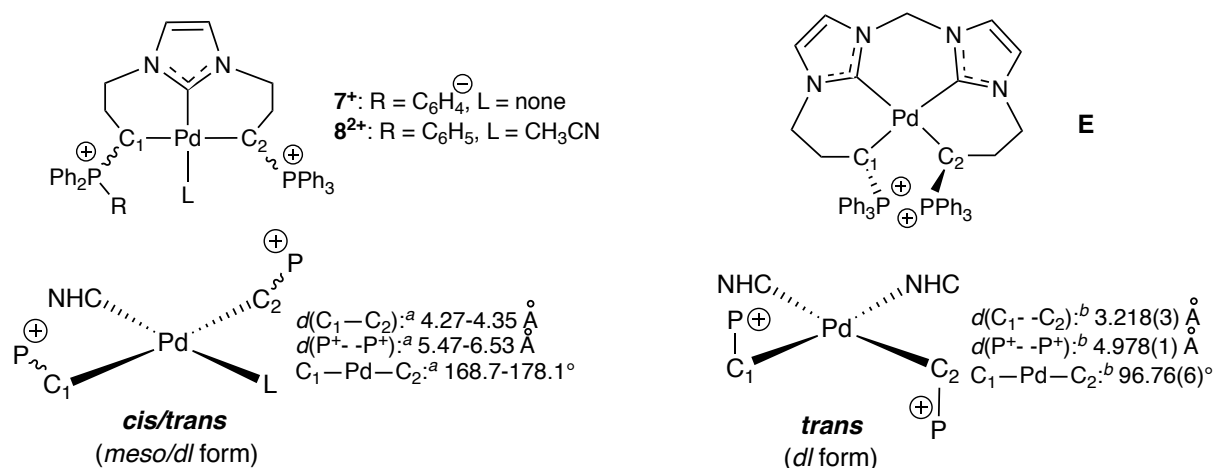


Figure 3. Perspective view of the cationic part of NHC, diphosphonium bis(ylide) Pd(II) complex *dl*-[**8**](OTf)₂ with thermal ellipsoids drawn at the 30% probability level. The H atoms are omitted for clarity, except those attached to the carbon atoms C6 and C9. Selected bond lengths [Å] and angles [°]: *dl*-[**8**](OTf)₂: C1–N1 = 1.36(1); C1–N2 = 1.34(2); C2–C3 = 1.39(3); C1–Pd1 = 1.89(1); C6–Pd1 = 2.156(9); C9–Pd1 = 2.12(1); N1–C1–N2 = 105.5(9); C1–Pd1–C6 = 89.8(4); C1–Pd1–C9 = 86.3(4); C6–Pd1–C9 = 173.2(4).



Scheme 4. Synthesis of the NHC, diphosphonium bis(ylide) Pd(II) pincer complex **[8](OTf)₂** from complex **[7](OTf)** (*left*), and substitution reactions at the Pd center of **[8](OTf)₂** with *t*-butyl isocyanide and carbon monoxide with respective formation of complexes **[9](OTf)₂** and **[10](OTf)₂** (*right*).

The diastereoselectivity of the formation of pincer **[8](OTf)₂** must be related to that of its *ortho*-metallated precursor **[7](OTf)**. In both cases, the diastereoselectivity can be tentatively rationalized by the existence of steric and electrostatic constraints between the PPh_3^+ substituents present at the C-ylidic positions. However, the present scenario has to be distinguished from the one recently reported concerning the diastereoselective formation of the Pd(II) complex **E** of a bis(NHC), diphosphonium bis(ylide) (Scheme 5, *right*).¹³ At first sight, the selectivity of the coordination process may be correlated with the distance occurring between the two bulky and cationic PPh_3^+ substituents. The shorter the distance between the cationic groups, the more the isomer (*trans*- or *dl* form) featuring the PPh_3^+ groups on either side of the coordination plane will be *a priori* favored. This specific situation was observed in the case of complex **E** ($d_{\text{C1-C2}} = 3.218(3) \text{ \AA}$, $d_{\text{P+-P+}} = 4.978(1) \text{ \AA}$) where steric and electrostatic repulsions were thus minimized.¹³ In contrast, a longer distance between the two cationic substituents ($d_{\text{C1-C2}} = 4.27\text{-}4.35 \text{ \AA}$, $d_{\text{P+-P+}} = 5.47\text{-}6.53 \text{ \AA}$) does not afford an efficient discrimination which causes the complex **[7](OTf)**, and consequently the complex **[8](OTf)₂** to be obtained as a 75/25 mixture of two diastereomers (*cis/trans* or *meso/dl* form) (Scheme 5, *left*).

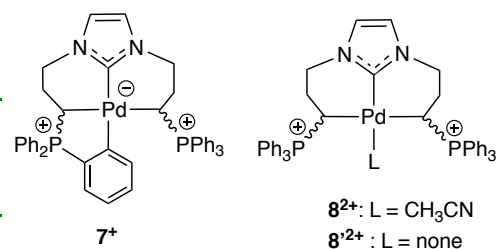


Scheme 5. Representations of the Pd square planar environment in NHC, diphosphonium bis(ylide) 7^+ , and 8^{2+} (left) and bis(NHC), diphosphonium bis(ylide) Pd(II) **E** complexes (right). The *cis* vs. *trans* denomination refers to the relative position of the PPh₃⁺ groups with respect to the Pd coordination plane.^a Calculated values determined from optimized geometries.^b Experimental values obtained from reference 13.

The relative stability of the diastereomers of the cationic Pd complexes 7^+ and 8^{2+} was investigated at the PBE-D3/6-31G**/LANL2DZ*(Pd) level of calculation both in vacuum or taking into account the acetonitrile solvent *via* a continuum dielectric medium as implemented in the PCM method (Table 1). The hypothetical T-shaped Pd complex 8^{2+} , in which the coordination site *trans* to the NHC is vacant was also considered at the same level of calculation in order to evaluate the role of the acetonitrile co-ligand.²⁸

Table 1. Relative energies of the *cis*- and *trans*- isomers of Pd pincer complexes 7^+ , 8^{2+} , and 8^{2+} calculated at the PBE-D3/6-31G**/LANL2DZ*(Pd) level of calculation (left).^a Schematic representation of NHC, bis(ylide) Pd complexes 7^+ , 8^{2+} , and 8^{2+} (right).^b

	PBE-D3	PCM-PBE-D3	ZPE ^c	Gibbs ^d
<i>cis</i> - 7^+ (RS/SR)	0.0	0.0	0.0	0.0
<i>trans</i> - 7^+ (RR/SS)	2.5	1.9	1.6	0.7
<i>cis</i> - 8^{2+} (meso)	0.7	0.1	0.03	0.0
<i>trans</i> - 8^{2+} (dl)	0.0	0.0	0.0	0.001
<i>cis</i> - 8^{2+} (meso)	3.9	0.0	0.4	2.0
<i>trans</i> - 8^{2+} (dl)	0.0	0.2	0.0	0.0



^a Energies are given in kcal/mol. PCM was used to take into account the acetonitrile solvent ($\epsilon = 35.688$).^b Optimized structures of complexes 7^+ , 8^{2+} , and $8'^{2+}$ are given in the supporting information.^c Zero-point corrected energies from PCM-PBE calculations.^d Gibbs free energies from PCM-PBE calculations.

The calculated relative energies are in agreement with the experimental observations that indicate in all cases the existence of two diastereomeric complexes. In vacuum as well as in the solvent phase, and whatever the calculation method, the two diastereomers of cationic complexes 7^+ and 8^{2+} were indeed calculated to be very close in energy with a difference lower than 2.5 kcal/mole. While in the *ortho*-metallated series (7^+), the *cis*-isomer appears to be the most stable isomer, in the bis-ylide series (8^{2+}), the two isomers are isoenergetic. It should be noted that at room temperature, the 75/25 ratio measured by NMR spectroscopy, corresponds to a Gibbs relative energy of about 0.65 kcal/mol, which is consistent with the Gibbs energy calculated for the *ortho*-metallated complex 7^+ (*ca.* 0.7 kcal/mol, see table 1). The slight deviation observed for complex 8^{2+} might be explained by its dicationic nature and the weak interaction between the metal and the CH₃CN molecule more difficult to describe. In any case, the quasi-degeneracy of the two diastereomers in both series suggests the moderate influence of steric and electrostatic constraints of the PPh₃⁺ substituents on the coordination selectivity. These findings are in favor of a thermodynamic control of the reaction process. For the T-shaped Pd complex $8'^{2+}$, the two isomers were also found to be close in energy, indicating that the acetonitrile ligand *trans* to the NHC exerts little influence (or any) on their relative energy.

Displacement of CH₃CN at the Pd center was then investigated in order to evaluate the stereo-electronic properties of this new category of pincer complexes. Treatment of bis(ylide) Pd complex **[8]**(OTf)₂ with *t*-butyl isocyanide in CH₂Cl₂ at -78 °C afforded the corresponding coordinated isocyanide adduct **[9]**(OTf)₂, isolated in 94% yield as a 75/25 mixture of diastereomers, a diastereomeric ratio similar to that of **[8]**(OTf)₂ (Scheme 4, *right*). Upon exchange of CH₃CN for *t*-BuNC, the ³¹P NMR spectrum remained essentially unchanged with the occurrence of two singlets (minor: δ_P 33.6, major: δ_P 34.6 ppm; **[8]**(OTf)₂: δ_P 32.7, 33.8 ppm). The ¹H NMR spectrum was consistent with the coordination of the isocyanide molecule as evidenced by the presence of two single resonances for the *t*-Bu group (major: δ_H 0.50, minor: δ_H 0.72 ppm). In the ¹³C NMR spectrum, the isocyanide carbon atom directly attached to the metal center was observed as a broad signal (major: δ_C 135.7, minor: δ_C 135.8 ppm), in

agreement with a η^1 coordination mode.²⁹ The IR spectrum revealed also the presence of a strong $\nu_{\text{C}=\text{N}}$ band at 2194 cm^{-1} in the typical range for coordinated isocyanides.³⁰

The structure of both diastereomers of complex **[9](OTf)₂** could be determined by X-ray diffraction analysis of pale yellow single crystals deposited from a $\text{CH}_2\text{Cl}_2/\text{Et}_2\text{O}$ solution mixture at room temperature, the crystals of the two diastereomers being separated manually (Figure 4, Table 2).²⁰ In both complexes, the Pd(II) atom being part of two strongly distorted fused six-membered metallacycles adopts a somewhat square planar environment, the phosphonium ylide ends being in a mutual *trans* arrangement ($\text{C6-Pd1-C9} = 165.42(11)^\circ$ and $170.1(3)^\circ$) and the *t*-butyl isocyanide ligand being located in *trans* position relative to the central NHC moiety ($\text{C1-Pd1-C46} = 174.65(13)^\circ$ and $168.7(3)^\circ$). As earlier pointed out, both ylidic C6 and C9 carbon atoms are stereogenic. In a first diastereomer, the two phosphonium fragments attached to those carbon atoms are nearly located on the same side on the C₄ coordination plane, conferring the $S_{\text{C6}}, R_{\text{C9}}$ ($R_{\text{C6}}, S_{\text{C9}}$) configuration to the *meso*-**[9](OTf)₂** complex (Figure 4, *left*). Conversely in the second diastereomer, the two phosphonium moieties are located on each side of the Pd coordination plane, the configuration of C6 and C9 carbon atoms being on that case $S_{\text{C6}}, S_{\text{C9}}$ ($R_{\text{C6}}, R_{\text{C9}}$), thus corresponding to the *dl*-**[9](OTf)₂** complex (Figure 4, *right*). It is therefore deduced that the flexibility of the two fused six-membered metallacycles makes it possible to locate the two groups PPh_3^+ on the same side or on each side of the Pd coordination plane, which goes along with the large distance observed between the two cationic fragments (*meso*-**[9](OTf)₂**: $d(\text{C6}--\text{C9}) = 4.277(5)\text{ \AA}$, $d(\text{P1}^+--\text{P2}^+) = 6.406(1)\text{ \AA}$; *dl*-**[9](OTf)₂**: $d(\text{C6}--\text{C9}) = 4.29(1)\text{ \AA}$, $d(\text{P1}^+--\text{P2}^+) = 6.292(3)\text{ \AA}$). The C–Pd bond distances involving the NHC and the ylide moieties (*meso*-**[9](OTf)₂**: $\text{C1-Pd1} = 1.960(3)\text{ \AA}$, $\text{C6-Pd1} = 2.169(3)\text{ \AA}$, $\text{C9-Pd1} = 2.143(3)\text{ \AA}$; *dl*-**[9](OTf)₂**: $\text{C1-Pd1} = 1.951(7)\text{ \AA}$, $\text{C6-Pd1} = 2.162(9)\text{ \AA}$, $\text{C9-Pd1} = 2.138(7)\text{ \AA}$) fall within the range of those reported in related Pd(II) complexes, with the $\text{Csp}^2\text{-Pd}$ bond being significantly shorter than the $\text{Csp}^3\text{-Pd}$ ones.¹²⁻¹³ The C–Pd bond distances of the coordinated isocyanide (*meso*-**[9](OTf)₂**: $\text{C46-Pd1} = 2.010(3)\text{ \AA}$; *dl*-**[9](OTf)₂**: $\text{C46-Pd1} = 2.013(9)\text{ \AA}$) fit into the domain of reported data ($1.979\text{--}2.038\text{ \AA}$) for this type of chemical bond.³¹ The deviation observed from the ideally linear Pd–CN*t*Bu coordination mode is likely caused by the steric demand of the PPh_3^+ groups (*meso*-**[9](OTf)₂**: $\text{C1-Pd1-C46} = 174.65(13)^\circ$; *dl*-**[9](OTf)₂**: $\text{C1-Pd1-C46} = 168.7(3)^\circ$).

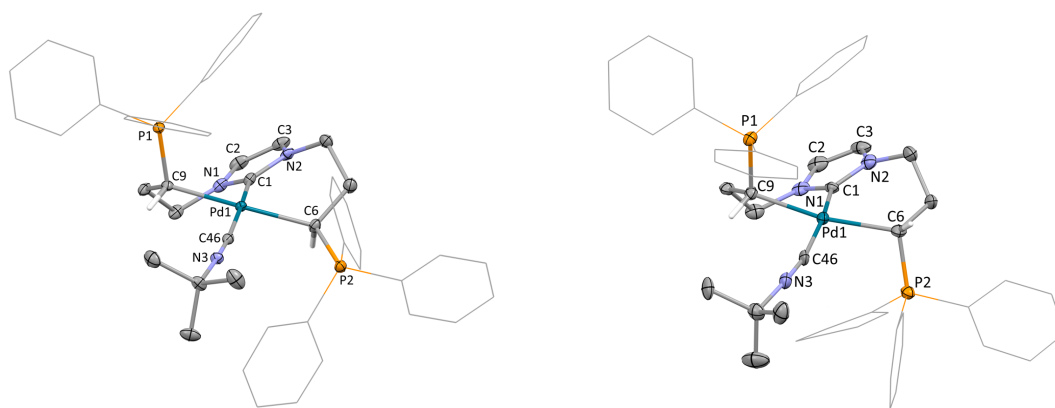


Figure 4. Perspective views of the cationic part of NHC, diphosphonium bis(ylide) Pd(II) complexes *meso*-[**9**](OTf)₂ (*left*), and *dl*-[**9**](OTf)₂ (*right*) with thermal ellipsoids drawn at the 30% probability level. The H atoms are omitted for clarity, except those attached to the carbon atoms C6 and C9.

Table 2. Selected bond distances [Å] and angles (°) for complexes *meso*-[**9**](OTf)₂ and *dl*-[**9**](OTf)₂ (Figure 4).^a Internuclear distances *d* determined with the Mercury interface.

	<i>meso</i> -[9](OTf) ₂	<i>dl</i> -[9](OTf) ₂
C1–N1	1.338(4)	1.351(11)
C1–N2	1.343(4)	1.352(10)
C1–Pd1	1.960(3)	1.951(7)
C6–Pd1	2.169(3)	2.162(9)
C9–Pd1	2.143(3)	2.138(7)
C46–Pd1	2.010(3)	2.013(9)
C46–N3	1.141(4)	1.126(10)
N1–C1–N2	107.0(3)	104.7(6)
C6–Pd1–C9	165.42(11)	170.1(3)
C1–Pd1–C46	174.65(13)	168.7(3)
C1–Pd1–C6	79.53(12)	87.2(3)
C1–Pd1–C9	86.74(12)	86.7(3)
Pd1–C46–N3	173.9(3)	166.7(7)
<i>d</i> (C6--C9) ^a	4.277(5)	4.29(1)
<i>d</i> (P1--P2) ^a	6.406(1)	6.292(3)

The preparation of carbon-based pincer Pd(II) carbonyl derivatives from **[8](OTf)₂** was then considered, having in mind that complexes of this type are rather scarce, and that strongly donor ancillary ligands are actually prone to stabilize them.³² Indeed, unlike many stable Ni,³³ Ir or Rh³⁴ carbonyl complexes, in the Pd series, the carbonyl ligand tends to easily dissociate due to the weak back-donation of the metal center.³⁵ Following a classical procedure, CO gas was bubbled through a solution of complex **[8](OTf)₂** in CH₂Cl₂ at room temperature (Scheme 4, *right*). ³¹P NMR monitoring indicated 90% conversion with the appearance of a set of two new single resonances (minor: δ_P 33.3, major: δ_P 35.7 ppm) for the two diastereomers of the Pd(II) carbonyl complex **[10](OTf)₂**, still present in a 75/25 ratio. The existence of the [Ph₃P⁺CH(R)]₂-Pd-CO arrangement was highlighted by ¹³C NMR spectroscopy with the presence of two deshielded signals (minor: δ_C 181.4 ppm (brs), major: δ_C 183.2 ppm (t, ³J_{CP} = 5.0 Hz)) for the CO fragment. The chemical shifts of carbenic and ylidic carbon atoms were not significantly affected by the nature of the L ligand within the series as illustrated by their respective ¹³C NMR resonances (**[8](OTf)₂** (L = CH₃CN): δ_{N_2C} 160.1, 161.4 ppm; δ_{PCH} 7.8, 9.9 ppm; **[9](OTf)₂** (L = *t*-BuNC): δ_{N_2C} 166.6, 168.0 ppm; δ_{PCH} 6.5, 7.0 ppm; **[10](OTf)₂** (L = CO): δ_{N_2C} 161.4 ppm (major), 165.4 ppm (minor); δ_{PCH} 9.9 ppm (major), 11.5 ppm (minor)). The characteristic IR ν_{CO} band was found at 2114 cm⁻¹. To our knowledge, the rare examples of reported pincer Pd(II) carbonyl complexes derived from POCOP,^{32a} P(NH)C(NH)P,^{32a} indenyl,^{32b} and indolyl^{32b} ligands are all characterized by the presence of two fused five-membered metallacycles. Since the complex **[10](OTf)₂** is the first example in the series featuring two fused six membered cycles, it would be risky to evaluate the donor character of the NHC, diphosphonium bis(ylide) ligand on the sole basis of the ν_{CO} frequency values, even if it is expected to act as strongly donor ligand.³⁶

Conclusion

A convenient two-step synthesis of a new class of imidazolium salt bearing two phosphonium chains **[3]X₃** (X = Br, OTf) was reported. The difference in acidity between the two cationic subunits allowed the selective preparation of bis(N-phosphonio)-(NHC) Pd(II) complexes **[4-5](OTf)₂**. On the way to a new family of LX₂-type pincer complexes, an original *ortho*-metallated Pd(II) complex **[7](OTf)** was isolated. The Pd(II) pincer complex **[8](OTf)₂** of an electron-rich C,C,C-NHC, diphosphonium bis(ylide) ligand was formed, thanks to the selective cleavage of the C_{ar}-Pd bond of complex **[7](OTf)**. The complex **[8](OTf)₂** was readily converted to analogous pincers **[9](OTf)₂** and **[10](OTf)₂** of the same family, through an efficient exchange reaction at the Pd center induced by addition of *t*-butyl isocyanide and carbon monoxide, respectively. The experimental diastereoisomeric excess (*de*

= 50%) observed for the formation of pincer-type complexes [7](OTf), and [8-10](OTf)₂ upon coordination of the two ylidic arms was rationalized by DFT calculations which confirmed in both cases the quasi-degeneracy of the *meso*- and *dl*- isomers. The availability of NHC, diphosphonium bis(ylide) pincer complexes on a gram scale as well as their air stability should favor future developments, especially in the field of homogeneous catalysis requiring very electron-rich ligands.

Experimental Section

General Remarks. All manipulations were performed under an inert atmosphere of dry nitrogen by using standard vacuum line and Schlenk tube techniques. Dry and oxygen-free organic solvents (THF, Et₂O, CH₂Cl₂, toluene, pentane) were obtained using a LabSolv (Innovative Technology) solvent purification system. Acetonitrile was dried and distilled over CaH₂ under argon. All other reagent-grade chemicals were purchased from commercial sources and used as received. Chromatographic purification was carried out on silica gel (SiO₂, 63–200 μm). ¹H, ³¹P, and ¹³C NMR spectra were obtained on Bruker Avance 400 and Avance III HD 400 spectrometers. NMR chemical shifts δ are in ppm, with positive values to high frequency relative to the tetramethylsilane reference for ¹H and ¹³C and to H₃PO₄ for ³¹P. If necessary, additional information on the carbon signal attribution was obtained using ¹³C{¹H, ³¹P}, *J*-modulated spin-echo (JMOD) ¹³C{¹H}, ¹H–¹³C HMQC, and/or HMBC experiments. Mass spectra (ESI mode) were obtained using a Xevo G2 QToF (Waters) spectrometer and were performed by the mass spectrometry service of the “Institut de Chimie de Toulouse”. Elemental analyses were carried out by the elemental analysis service of the LCC using a PerkinElmer 2400 series II analyzer. Cyclic voltammetric measurements were carried out by the electrochemistry service of the LCC using a Autolab PGSTAT100 potentiostat controlled by GPES 4.09 software.

Synthesis of [2]Br

Imidazole **1** (1.00 g, 14.69 mmol) and (3-bromopropyl)triphenylphosphonium bromide (3.26 g, 6.99 mmol) were heated at 120 °C in C₆H₅Cl (30 mL) for 15 hours. After evaporation of the solvent, the crude residue was washed with a saturated aqueous NaHCO₃ solution (40 mL). The organic layer was extracted several times with CH₂Cl₂ (3 x 80 mL) and dried over Na₂SO₄. After evaporation of the solvent, [2]Br was obtained as a white powder (2.07 g, 66%). Recrystallization from CH₃CN at room temperature gave colorless crystals (Mp = 156–158 °C). ³¹P{¹H} NMR (162 MHz, CDCl₃, 25 °C): δ = 23.9 (s); ¹H NMR (400 MHz, CD₃CN, 25 °C) δ = 7.83–7.89 (m, 3H, CH_{Ph}), 7.64–7.73 (m, 12H, CH_{Ph}), 7.52 (s, 1H, N₂CH),

7.02 (s, 1H, CH_{Im}), 6.93 (s, 1H, CH_{Im}), 4.13–4.18 (m, 2H, NCH₂), 3.18–3.28 (m, 2H, PCH₂), 2.02–2.09 (m, 2H, CH₂); ¹³C{¹H} NMR (100.6 MHz, CDCl₃, 25 °C): δ = 137.5 (s, N₂CH), 135.2 (d, *J*_{CP} = 3.0 Hz, CH_{Ph}), 133.5 (d, *J*_{CP} = 9.8 Hz, CH_{Ph}), 130.5 (d, *J*_{CP} = 12.8 Hz, CH_{Ph}), 129.3 (s, CH_{Im}), 119.3 (s, CH_{Im}), 117.5 (d, *J*_{CP} = 86.0 Hz, C_{Ph}), 45.8 (d, *J*_{CP} = 19.6 Hz, NCH₂), 24.9 (d, *J*_{CP} = 3.0 Hz, CH₂), 19.7 (d, *J*_{CP} = 53.6 Hz, PCH₂). MS (ES⁺): *m/z*: 371.3 [M – Br]⁺; elemental analysis for C₂₄H₂₄BrN₂P·0.5H₂O: calcd, C 62.62, H 5.47, N 6.09; found, C 62.51, H 5.27, N 6.24.

Synthesis of [3]Br₃

Imidazole [2]Br (1.20 g, 2.66 mmol) and (3-bromopropyl)triphenylphosphonium bromide (1.37 g, 2.95 mmol) were stirred at 120 °C in DMF (40 mL) for 12 hours. After evaporation of the solvent, the solid residue was recrystallized in a minimum amount of CH₃CN (10 mL). After filtration of the solution, [3]Br₃ was obtained as a white powder (2.19 g, 90%; Mp = 184–186 °C). Despite the repetition of the crystallization step (3 times), residual traces of DMF were still observed. ³¹P{¹H} NMR (162 MHz, CDCl₃, 25 °C): δ = 24.7 (s); ¹H NMR (400 MHz, CDCl₃, 25 °C): δ = 10.11 (brs, 1H, N₂CH), 7.62–7.96 (m, 32H, CH_{Ph}, CH_{Im}), 4.88 (t, *J*_{HH} = 6.9 Hz, 4H, NCH₂), 4.02–4.09 (m, 4H, PCH₂), 2.29–2.35 (m, 4H, CH₂); ¹³C{¹H} NMR (100.6 MHz, CDCl₃, 25 °C): δ = 136.4 (s, N₂CH), 135.1 (d, *J*_{CP} = 3.0 Hz, CH_{Ph}), 134.0 (d, *J*_{CP} = 10.3 Hz, CH_{Ph}), 130.6 (d, *J*_{CP} = 12.7 Hz, CH_{Ph}), 123.2 (s, CH_{Im}), 117.6 (d, *J*_{CP} = 86.6 Hz, C_{Ph}), 48.9 (d, *J*_{CP} = 20.7 Hz, NCH₂), 24.0 (d, *J*_{CP} = 2.6 Hz, CH₂), 20.1 (d, *J*_{CP} = 53.2 Hz, PCH₂); MS (ES⁺): *m/z*: 834.9 [M – Br]⁺; elemental analysis for C₄₅H₄₅Br₃N₂P₂·0.3DMF·2.5H₂O: calcd, C 56.11, H 5.34, N 3.28; found, C 55.88, H 5.06, N 3.37.

Synthesis of [3](OTf)₃

[3]Br₃ (2.43 g, 2.66 mmol) and sodium trifluoromethanesulfonate (1.60 g, 9.32 mmol) were dissolved in CH₂Cl₂ (60 mL) and the solution was stirred at room temperature for 12 hours. After evaporation of the solvent, the crude residue was washed with water (30 mL). The organic layer was extracted with CH₂Cl₂ (2 x 30 mL) and dried over Na₂SO₄. After evaporation of the solvent, [3](OTf)₃ was obtained as a white powder (2.60 g, 87%). Recrystallization from THF/pentane at room temperature gave colorless crystals (Mp = 86–88 °C). ³¹P{¹H} NMR (162 MHz, CD₃CN, 25 °C): δ = 23.7 (s); ¹H NMR (400 MHz, CD₃CN, 25 °C): δ = 8.87 (brs, 1H, N₂CH), 7.84–7.91 (m, 5H, CH_{Ph}), 7.65–7.79 (m, 25H, CH_{Ph}), 7.48 (brs, 2H, CH_{Im}), 4.40 (t, *J*_{HH} = 7.0 Hz, 4H, NCH₂), 3.32–3.40 (m, 4H, PCH₂), 2.15–2.24 (m, 4H, CH₂); ¹³C{¹H} NMR (100.6 MHz, CD₃CN, 25 °C): δ = 137.4 (s, N₂CH), 136.2 (d, *J*_{CP} =

3.1 Hz, CH_{Ph}), 134.7 (d, $J_{CP} = 10.0$ Hz, CH_{Ph}), 131.3 (d, $J_{CP} = 12.4$ Hz, CH_{Ph}), 123.7 (s, CH_{Im}), 122.0 (q, $J_{CF} = 321.2$ Hz, CF₃), 118.6 (d, $J_{CP} = 87.5$ Hz, C_{Ph}), 49.9 (d, $J_{CP} = 21.1$ Hz, NCH₂), 23.9 (d, $J_{CP} = 2.6$ Hz, CH₂), 19.9 (d, $J_{CP} = 54.8$ Hz, PCH₂). MS (ES⁺): m/z : 973.2 [M – CF₃SO₃]⁺; elemental analysis for C₄₈H₄₅F₉N₂O₉P₂S₃: calcd, C 51.34, H 4.04, N 2.49; found, C 51.07, H 3.71, N 2.55.

Synthesis of [4](OTf)₂

A mixture of [Pd(allyl)Cl]₂ (0.08 g, 0.22 mmol), [3](OTf)₃ (0.50 g, 0.44 mmol) and anhydrous K₂CO₃ (0.09 g, 0.66 mmol) was dissolved in CH₃CN (20 mL) and stirred at room temperature for 15 hours. After filtration over Celite and evaporation of the solvent, [4](OTf)₂ was obtained as a white powder (0.48 g, 94%). Recrystallization from CH₃CN/Et₂O at room temperature gave pale yellow crystals (Mp = 110–112 °C). ³¹P{¹H} NMR (162 MHz, CD₃CN, 25 °C): $\delta = 23.8$ (s); ¹H NMR (400 MHz, CD₃CN, 25 °C): $\delta = 7.79$ – 7.85 (m, 5H, CH_{Ph}), 7.63–7.75 (m, 25H, CH_{Ph}), 7.18 (s, 2H, CH_{Im}), 5.24 (m, 1H, CH_{allyl}), 4.24–4.36 (m, 4H, NCH₂), 4.07 (d, $J_{HH} = 7.6$ Hz, 1H, CH_{2allyl}), 3.32–3.44 (m, 4H, PCH₂), 3.25–3.32 (m, 1H, CH_{2allyl}), 3.11 (d, $J_{HH} = 13.6$ Hz, 1H, CH_{2allyl}), 2.31 (brd, $J_{HH} = 11.9$ Hz, 1H, CH_{2allyl}), 2.12–2.20 (m, 4H, CH₂); ¹³C{¹H} NMR (100.6 MHz, CD₃CN, 25 °C): $\delta = 180.9$ (s, N₂C), 136.1 (d, $J_{CP} = 3.0$ Hz, CH_{Ph}), 134.6 (d, $J_{CP} = 10.0$ Hz, CH_{Ph}), 131.2 (d, $J_{CP} = 12.9$ Hz, CH_{Ph}), 123.1 (s, CH_{Im}), 122.0 (q, $J_{CF} = 319.9$ Hz, CF₃), 119.0 (d, $J_{CP} = 86.7$ Hz, C_{Ph}), 116.4 (s, CH_{allyl}), 72.6 (s, CH_{2allyl}), 51.1 (d, $J_{CP} = 18.9$ Hz, NCH₂), 49.9 (s, CH_{2allyl}), 24.9 (d, $J_{CP} = 3.1$ Hz, CH₂), 20.2 (d, $J_{CP} = 53.6$ Hz, PCH₂). MS (ES⁺): m/z : 1119.1 [M – Cl]⁺; elemental analysis for C₅₀H₄₉ClF₆N₂O₆P₂PdS₂: calcd, C 51.96, H 4.27, N 2.42; found, C 51.53, H 3.52, N 2.59.

Synthesis of [5](OTf)₂

A mixture of [3](OTf)₃ (0.31 g, 0.27 mmol), PdCl₂ (0.048 g, 0.27 mmol), anhydrous K₂CO₃ (0.18 g, 1.35 mmol), and pyridine (65.3 μ L, 0.81 mmol) was stirred at room temperature in CH₃CN (15 mL) for 12 hours. After filtration over Celite and evaporation of the solvent under vacuum, [5](OTf)₂ was obtained as a pale yellow powder (0.26 g, 78%). Recrystallization from CH₃CN/Et₂O at –20 °C gave pale yellow crystals (Mp = 198–200 °C). ³¹P{¹H} NMR (162 MHz, CD₃CN, 25 °C): $\delta = 23.7$ (s); ¹H NMR (400 MHz, CD₃CN, 25 °C): $\delta = 8.71$ (m, 2H, CH_{Py}), 7.97 (tt, $J_{HH} = 1.7, 7.6$ Hz, 1H, CH_{Py}), 7.79–7.85 (m, 5H, CH_{Ph}), 7.59–7.74 (m, 25H, CH_{Ph}), 7.48 (m, 2H, CH_{Py}), 7.15 (s, 2H, CH_{Im}), 4.71 (t, $J_{HH} = 6.6$ Hz, 4H, NCH₂), 3.46–3.54 (m, 4H, PCH₂), 2.40–2.50 (m, 4H, CH₂); ¹³C{¹H} NMR (100.6 MHz, CD₃CN, 25 °C): $\delta = 152.0$ (s, CH_{Py}), 150.7 (s, N₂C), 140.0 (s, CH_{Py}), 136.2 (d, $J_{CP} = 3.0$ Hz, CH_{Ph}), 134.7 (d, $J_{CP} = 10.3$ Hz, CH_{Ph}), 131.3 (d, $J_{CP} = 12.4$ Hz, CH_{Ph}), 125.9 (s, CH_{Py}), 124.1 (s, CH_{Im}), 122.2 (q,

$J_{CF} = 319.9$ Hz, CF_3), 118.9 (d, $J_{CP} = 86.9$ Hz, C_{Ph}), 51.0 (d, $J_{CP} = 19.2$ Hz, NCH_2), 24.6 (d, $J_{CP} = 3.1$ Hz, CH_2), 20.5 (d, $J_{CP} = 53.9$ Hz, PCH_2). MS (ES^+): m/z : 1078.1 [$M - CF_3SO_3$] $^+$; elemental analysis for $C_{52}H_{49}Cl_2F_6N_3O_6P_2PdS_2$: calcd, C 50.80, H 4.02, N 3.42; found, C 50.69, H 3.70, N 3.45.

Synthesis of [6](OTf)₂

A 1/1 mixture of *t*BuOK (0.061 g, 0.54 mmol) and complex [4](OTf)₂ (0.60 g, 0.52 mmol) was cooled to -78 °C and THF (10 mL) was added. The suspension was warmed to room temperature and stirred for 2 hours. After evaporation of the solvent, the solid residue was dissolved in CH_2Cl_2 (10 mL) and filtered over Celite. After purification by chromatography on silica gel (AcOEt/MeOH), [6](OTf)₂ was obtained as a yellow solid (0.40 g, 70%), and as a mixture of two diastereoisomers (60/40); (Mp = 110–112 °C). NMR assignment: ^amajor isomer (60%); ^bminor isomer (40%): ³¹P{¹H} NMR (162 MHz, CD_3CN , 25 °C): $\delta = 32.2^b$ (s), 23.8^b (s); 31.4^a (s), 23.7^a (s); ¹H NMR (400 MHz, CD_3CN , 25 °C): $\delta = 7.47$ – $7.90^{a,b}$ (m, 75H, CH_{Ph}), 7.10^a (d, $J_{HH} = 1.8$ Hz, 1.5H, CH_{Im}), 7.05^a (d, $J_{HH} = 1.8$ Hz, 1.5H, CH_{Im}), 6.97^b (d, $J_{HH} = 1.8$ Hz, 1H, CH_{Im}), 6.95^b (d, $J_{HH} = 1.8$ Hz, 1H, CH_{Im}), 4.81–4.92^{a,b} (m, 2.5H, CH_{allyl}), 3.21–4.20^{a,b} (m, CH_2 , CH_{2allyl} , 22H), 2.91^b (d, $J_{HH} = 7.2$ Hz, 1H, CH_{2allyl}), 2.51^a (d, $J_{HH} = 12.8$ Hz, 1.5H, CH_{2allyl}), 2.30–2.42^{a,b} (m, CH_2 , 2.5H), 2.25^a (d, $J_{HH} = 7.4$ Hz, 1.5H, CH_{2allyl}), 2.13^a (d, $J_{HH} = 13.8$ Hz, 1.5H, CH_{2allyl}), 2.10^b (d, $J_{HH} = 13.5$ Hz, 1H, CH_{2allyl}), 1.90–2.05^{a,b} (m, CH_2 , 2.5H), 1.52–1.75^{a,b} (m, PCH, 2.5H), 1.50^a (d, $J_{HH} = 13.2$ Hz, 1.5H, CH_{allyl}); ¹³C{¹H} NMR (100.6 MHz, CD_3CN , 25 °C): $\delta = 179.1^a$ (s, N_2C), 178.3^b (s, N_2C), 136.3^a (d, $J_{CP} = 3.1$ Hz, CH_{Ph}), 136.1^b (d, $J_{CP} = 3.0$ Hz, CH_{Ph}), 134.7^a (d, $J_{CP} = 10.0$ Hz, CH_{Ph}), 134.4^b (d, $J_{CP} = 8.6$ Hz, CH_{Ph}), 134.2^b (d, $J_{CP} = 9.0$ Hz, CH_{Ph}), 134.0^a (d, $J_{CP} = 3.0$ Hz, CH_{Ph}), 131.4^a (d, $J_{CP} = 12.7$ Hz, CH_{Ph}), 131.3^b (d, $J_{CP} = 12.7$ Hz, CH_{Ph}), 130.2^b (d, $J_{CP} = 11.5$ Hz, CH_{Ph}), 130.0^a (d, $J_{CP} = 11.5$ Hz, CH_{Ph}), 126.2^b (d, $J_{CP} = 83.5$ Hz, C_{Ph}), 126.0^a (d, $J_{CP} = 83.7$ Hz, C_{Ph}), 123.1^a (s, CH_{Im}), 122.7^b (s, CH_{Im}), 122.1 (q, $J_{CF} = 320.9$ Hz, CF_3), 121.0^a (s, CH_{Im}), 120.5^b (s, CH_{Im}), 118.81^a (d, $J_{CP} = 88.5$ Hz, C_{Ph}), 118.77^b (d, $J_{CP} = 90.5$ Hz, C_{Ph}), 118.5^b (s, CH_{allyl}), 117.6^a (s, CH_{allyl}), 63.2^a (s, CH_{2allyl}), 61.8^b (s, CH_{2allyl}), 57.2^b (s, CH_{2allyl}), 56.1^a (s, CH_{2allyl}), 54.1^a (d, $J_{CP} = 17.4$ Hz, NCH_2), 53.8^b (d, $J_{CP} = 18.8$ Hz, NCH_2), 51.5^b (d, $J_{CP} = 21.2$ Hz, NCH_2), 51.2^a (d, $J_{CP} = 21.1$ Hz, NCH_2), 27.4^a (s, CH_2), 27.2^b (s, CH_2), 24.8^b (d, $J_{CP} = 3.8$ Hz, CH_2), 24.7^a (d, $J_{CP} = 3.8$ Hz, CH_2), 20.2^b (d, $J_{CP} = 54.4$ Hz, PCH_2), 20.1^a (d, $J_{CP} = 54.4$ Hz, PCH_2), 2.1^a (d, $J_{CP} = 34.2$ Hz, PCH), 2.0^b (d, $J_{CP} = 33.2$ Hz, PCH); MS (ES^+): m/z : 969.2 [$M - CF_3SO_3$] $^+$; HRMS (ES^+): calcd for $C_{49}H_{48}F_3N_2O_3P_2PdS$, 969.1865; found, 969.1866; elemental analysis for $C_{50}H_{48}F_6N_2O_6P_2PdS_2 \cdot 2.0H_2O$: calcd, C 51.97, H 4.54, N 2.42; found, C 51.60, H 3.40, N 2.32.

Synthesis of [7](OTf)

1st method: [5](OTf)₂ (0.31 g, 0.25 mmol) and anhydrous Cs₂CO₃ (0.24 g, 0.75 mmol) were dissolved in CH₃CN (15 mL), and the suspension was stirred at 70 °C for 12 hours. After filtration over Celite, the solvent was evaporated under vacuum. The crude residue was dissolved in CH₂Cl₂ (10 mL), and the solution was filtered over Celite. After evaporation of the solvent, [7](OTf) was obtained as a pale yellow powder (0.20 g, 86%), and as a mixture of two diastereoisomers (75/25); (Mp = 158–160°C).

2nd method: A mixture of [3](OTf)₃ (0.10 g, 0.09 mmol), PdCl₂ (0.016 g, 0.09 mmol), and anhydrous Cs₂CO₃ (0.13 g, 0.45 mmol) was stirred at 70 °C in CH₃CN (8 mL) for 12 hours. After filtration over Celite and evaporation of the solvent under vacuum, the crude residue was dissolved in CH₂Cl₂ (10 mL), and the solution was filtered over Celite. After evaporation of the solvent, [7](OTf) was obtained as a pale yellow powder (0.05 g, 65%), and as a mixture of two diastereoisomers (75/25). NMR assignment: ^amajor isomer (75%); ^bminor isomer (25%): ³¹P{¹H} NMR (162 MHz, CD₃CN, 25 °C): δ = 29.2^a (brs), 28.2^a (brs); 31.1^b (s), 23.3^b (s); ¹H NMR (400 MHz, CD₃CN, 25 °C): ^amajor isomer: δ 8.27 (d, *J* = 7.4 Hz, 1H, CH_{Ph-ortho}), 7.51–7.71 (m, 12H, CH_{Ph}), 7.44–7.47 (m, 3H, CH_{Ph}), 7.32–7.36 (m, 1H, CH_{Ph}), 7.30 (td, *J* = 1.4, 7.5 Hz, 1H, CH_{Ph-ortho}), 7.15–7.29 (m, 9H, CH_{Ph}), 7.00 (t, *J* = 7.5 Hz, 1H, CH_{Ph-ortho}), 6.84 (d, *J* = 7.6 Hz, 1H, CH_{Ph-ortho}), 6.59 (d, *J* = 1.8 Hz, 1H, CH_{Im}), 6.43 (d, *J* = 1.8 Hz, 1H, CH_{Im}), 4.00–4.04 (m, 1H, NCH₂), 3.84–3.89 (m, 1H, NCH₂), 3.67–3.71 (m, 1H, NCH₂), 3.31 (t, *J* = 4.7 Hz, 1H, PCH), 3.12–3.19 (m, 1H, CH₂), 2.99–3.04 (m, 1H, NCH₂), 2.79–2.84 (m, 1H, CH₂), 2.40–2.45 (m, 2H, CH₂, PCH), 1.90–1.95 (m, 1H, CH₂). ^bminor isomer: δ 7.10–7.89 (m, 25H, CH_{Ph}), 6.98 (m, 1H, CH_{Ph-ortho}), 6.83 (m, 1H, CH_{Ph-ortho}), 6.74 (m, 1H, CH_{Ph-ortho}), 6.65 (m, 1H, CH_{Ph-ortho}), 6.62 (d, *J* = 1.8 Hz, 1H, CH_{Im}), 6.51 (d, *J* = 1.8 Hz, 1H, CH_{Im}), 3.90–3.95 (m, 2H, NCH₂), 3.50–3.60 (m, 2H, NCH₂), 3.23 (m, 1H, PCH), 3.10 (m, 1H, PCH), 2.30–2.50 (m, 4H, CH₂). ¹³C NMR (100.6 MHz, CD₃CN, 25 °C) δ = 183.5^a (d, *J*_{CP} = 36.2 Hz, C_{Ph-ortho}), 180.7^b (d, *J*_{CP} = 33.2 Hz, C_{Ph-ortho}), 178.8^b (brs, N₂C), 175.5^a (brs, N₂C), 139.9^b (d, *J*_{CP} = 116.7 Hz, C_{Ph-ipso}), 138.9^a (d, *J*_{CP} = 116.7 Hz, C_{Ph-ipso}), 138.8^a (d, *J*_{CP} = 20.1 Hz, CH_{Ph}), 137.6^b (d, *J*_{CP} = 19.1 Hz, CH_{Ph}), 135.6 (d, *J*_{CP} = 8.0 Hz, CH_{Ph}), 134.6 (d, *J*_{CP} = 8.0 Hz, CH_{Ph}), 134.5 (d, *J*_{CP} = 9.0 Hz, CH_{Ph}), 134.4 (d, *J*_{CP} = 9.0 Hz, CH_{Ph}), 134.3 (d, *J*_{CP} = 8.0 Hz, CH_{Ph}), 133.74 (d, *J*_{CP} = 8.0 Hz, CH_{Ph}), 133.71 (d, *J*_{CP} = 9.0 Hz, CH_{Ph}), 133.6 (d, *J*_{CP} = 3.0 Hz, CH_{Ph}), 133.5 (d, *J*_{CP} = 3.0 Hz, CH_{Ph}), 133.4 (d, *J*_{CP} = 3.0 Hz, CH_{Ph}), 133.2 (d, *J*_{CP} = 3.0 Hz, CH_{Ph}), 132.9 (d, *J*_{CP} = 3.0 Hz, CH_{Ph}), 131.2 (d, *J*_{CP} = 10.1 Hz, CH_{Ph}), 131.1 (d, *J*_{CP} = 8.0 Hz, CH_{Ph}), 131.0 (d, *J*_{CP} = 20.1 Hz, CH_{Ph}), 130.4 (d, *J*_{CP} = 10.1 Hz, CH_{Ph}), 130.3 (d, *J*_{CP} = 10.1 Hz, CH_{Ph}), 130.1 (d, *J*_{CP} = 11.1 Hz, CH_{Ph}), 129.6 (d, *J*_{CP} = 4.0 Hz, CH_{Ph}), 129.51 (d, *J*_{CP} = 11.1 Hz, CH_{Ph}), 129.48 (d, *J*_{CP} = 11.1 Hz, CH_{Ph}), 129.2 (d, *J*_{CP} = 11.1 Hz, CH_{Ph}), 126.3 (d, *J*_{CP} =

80.5 Hz, C_{Ph}), 126.1 (d, $J_{CP} = 82.5$ Hz, C_{Ph}), 124.5^a (d, $J_{CP} = 13.1$ Hz, CH_{Ph}), 124.2^b (d, $J_{CP} = 13.1$ Hz, CH_{Ph}), 122.0^{a,b} (q, $J_{CF} = 319.9$ Hz, CF₃), 121.5^a (s, CH_{Im}), 121.1^b (s, CH_{Im}), 120.6^a (s, CH_{Im}), 120.1^b (s, CH_{Im}), 53.2^b (d, $J_{CP} = 23.1$ Hz, NCH₂), 52.0^a (d, $J_{CP} = 3.0$ Hz, NCH₂), 51.3^b (d, $J_{CP} = 9.0$ Hz, NCH₂), 49.7^a (d, $J_{CP} = 6.0$ Hz, NCH₂), 27.5^a (d, $J_{CP} = 5.0$ Hz, CH₂), 26.5^b (d, $J_{CP} = 2.0$ Hz, CH₂), 26.3^b (s, CH₂), 26.1^a (d, $J_{CP} = 2.0$ Hz, CH₂), 18.4^b (d, $J_{CP} = 42.2$ Hz, PCH), 17.6^a (d, $J_{CP} = 37.2$ Hz, PCH), 11.0^b (dd, $J_{CP} = 2.0, 26.2$ Hz, PCH), 10.5^a (dd, $J_{CP} = 3.0, 21.1$ Hz, PCH). MS (ES⁺): m/z : 777.2 [M - CF₃SO₃]⁺; HRMS (ES⁺): calcd for C₄₅H₄₁N₂P₂Pd 777.1796; found, 777.1800; elemental analysis for C₄₆H₄₁F₃N₂O₃P₂PdS₂: calcd, C 59.58, H 4.46, N 3.02; found, C 59.57, H 4.28, N 3.07.

Synthesis of [8](OTf)₂

TfOH (0.5 M in CH₃CN, 0.65 mL, 0.32 mmol) was added at -40 °C to a solution of complex [7](OTf) (0.30 g, 0.32 mmol) in CH₃CN (10 mL). The mixture was warmed to room temperature for 2 hours. After filtration over Celite, the solvent was removed under vacuum, and complex [8](OTf)₂ was obtained as a pale yellow powder (0.39 g, 94%), and as a mixture of two diastereoisomers (75/25). Recrystallization from CH₂Cl₂/Et₂O at room temperature gave pale yellow crystals (Mp = 148–150 °C). NMR assignment: ^amajor isomer (75%); ^bminor isomer (25%): ³¹P{¹H} NMR (162 MHz, CD₃CN, 25 °C): δ = 33.8^a (s), 32.7^b (s); ¹H NMR (400 MHz, CD₃CN, 25 °C) δ = 7.53–7.72^{a,b} (m, 124.5H, CH_{Ph}), 6.96^a (s, 6.3H, CH_{Im}), 6.84^b (s, 2H, CH_{Im}), 3.99–4.05^{a,b} (m, 14.6H, NCH₂), 3.38^b (td, $J = 4.0, 12.0$ Hz, 2H, NCH₂), 3.25^b (q, $J = 8.0$ Hz, 2H, PCH), 2.58–2.66^a (m, 6.3H, PCH), 2.23–2.33^b (m, 2H, CH₂), 1.98–2.15^a (m, 12.6H, CH₂), 1.52–1.67^b (m, 2H, CH₂); ¹³C{¹H} NMR (100.6 MHz, CD₃CN, 25 °C) δ = 161.4^b (s, N₂C), 160.1^a (s, N₂C), 134.7^b (d, $J_{CP} = 9.1$ Hz, CH_{Ph}), 134.5^a (d, $J_{CP} = 8.8$ Hz, CH_{Ph}), 134.4^a (d, $J_{CP} = 3.0$ Hz, CH_{Ph}), 134.3^b (d, $J_{CP} = 3.0$ Hz, CH_{Ph}), 130.4^a (d, $J_{CP} = 11.6$ Hz, CH_{Ph}), 130.3^b (d, $J_{CP} = 11.9$ Hz, CH_{Ph}), 124.9^b (d, $J_{CP} = 82.5$ Hz, C_{Ph}), 124.7^a (d, $J_{CP} = 83.5$ Hz, C_{Ph}), 122.2^{a,b} (q, $J_{CF} = 320.9$ Hz, CF₃), 122.1^a (s, CH_{Im}), 121.9^b (s, CH_{Im}), 52.5^b (d, $J_{CP} = 14.7$ Hz, NCH₂), 51.9^a (d, $J_{CP} = 15.6$ Hz, NCH₂), 26.1^b (s, CH₂), 25.3^a (s, CH₂), 9.9^b (d, $J_{CP} = 32.8$ Hz, PCH), 7.8^a (d, $J_{CP} = 30.9$ Hz, PCH). MS (ES⁺): m/z : 927.1 [M - (CF₃SO₃ + CH₃CN)]⁺; HRMS (ES⁺): calcd for C₄₆H₄₂F₃N₂O₃P₂PdS, 927.1394; found, 927.1393; elemental analysis for C₄₉H₄₅F₆N₃O₆P₂PdS₂: calcd, C 52.62, H 4.06, N 3.76; found, C 52.03, H 3.66, N 3.35.

Synthesis of [9](OTf)₂

t-butyl isocyanide (27.3 μL, 0.24 mmol) was added at -78 °C to a solution of complex [8](OTf)₂ (0.18 g, 0.16 mmol) in CH₂Cl₂ (10 mL). The mixture was warmed to room

temperature for 2 hours. After filtration over Celite, the solvent was removed under vacuum, and complex [9](OTf)₂ was obtained as a pale yellow powder (0.17 g, 94 %), and as a mixture of two diastereoisomers (75/25). Recrystallization from CH₂Cl₂/Et₂O at room temperature gave pale yellow crystals (Mp = 186–188 °C). IR (CH₂Cl₂): $\nu_{C\equiv N}$ = 2194 cm⁻¹; NMR assignment: ^amajor isomer (75%); ^bminor isomer (25%): ³¹P{¹H} NMR (162 MHz, CD₂Cl₂, 25 °C): δ = 34.6^a (s), 33.6^b (s); ¹H NMR (400 MHz, CD₂Cl₂, 25 °C): δ = 7.57–7.75^{a,b} (m, 124.5H, CH_{Ph}), 6.96^a (s, 6.3H, CH_{Im}), 6.66^b (s, 2H, CH_{Im}), 3.95–4.12^a (m, 12.6H, NCH₂), 3.88–3.96^b (m, 2H, NCH₂), 3.62–3.70^b (m, 2H, PCH), 3.32–3.40^b (m, 2H, NCH₂), 2.67–2.75^a (m, 6.3H, PCH), 2.46–2.54^b (m, 2H, CH₂), 2.18–2.38^a (m, 12.6H, CH₂), 1.65–1.75^b (m, 2H, CH₂), 0.72^b (s, 9H, *t*Bu), 0.50^a (s, 28.35H, *t*Bu); ¹³C{¹H} NMR (100.6 MHz, CD₂Cl₂, 25 °C): δ = 168.0^b (s, N₂C), 166.6^a (s, N₂C), 135.8^b (brs, CN), 135.7^a (brs, CN), 134.4^a (d, J_{CP} = 3.1 Hz, CH_{Ph}), 134.3^b (d, J_{CP} = 8.6 Hz, CH_{Ph}), 134.2^a (d, J_{CP} = 8.6 Hz, CH_{Ph}), 134.0^b (d, J_{CP} = 2.9 Hz, CH_{Ph}), 130.3^a (d, J_{CP} = 11.5 Hz, CH_{Ph}), 130.2^b (d, J_{CP} = 11.7 Hz, CH_{Ph}), 124.2^b (d, J_{CP} = 82.9 Hz, C_{Ph}), 124.0^a (d, J_{CP} = 83.4 Hz, C_{Ph}), 121.9^a (s, CH_{Im}), 121.6^{a,b} (q, J_{CF} = 321.8 Hz, CF₃), 120.9^b (s, CH_{Im}), 58.5^a (s, C(CH₃)₃), 58.2^b (s, C(CH₃)₃), 52.0^b (d, J_{CP} = 13.7 Hz, NCH₂), 51.4^a (d, J_{CP} = 13.8 Hz, NCH₂), 29.4^b (s, CH₃), 29.1^a (s, CH₃), 26.5^b (s, CH₂), 25.4^a (s, CH₂), 7.0^b (d, J_{CP} = 32.8 Hz, PCH), 6.5^a (d, J_{CP} = 32.6 Hz, PCH). MS (ES⁺): *m/z*: 1010.2 [M – CF₃SO₃]⁺; elemental analysis for C₅₂H₅₁F₆N₃O₆P₂PdS₂0.3CH₂Cl₂: calcd, C 52.97, H 4.39, N 3.54; found, C 52.97, H 4.41, N 3.75.

Synthesis of [10](OTf)₂

[8](OTf) (0.05 g, 0.04 mmol) was dissolved in CD₂Cl₂ (0.5 mL) in a NMR tube, and carbon monoxide was bubbled during 15 min. A 90% conversion was observed by ³¹P NMR spectroscopy. Complex [10](OTf)₂ was fully characterized in solution as a mixture of two diastereoisomers (75/25). IR (CH₂Cl₂): ν_{CO} = 2114 cm⁻¹; NMR assignment: ^amajor isomer (75%); ^bminor isomer (25%): ³¹P{¹H} NMR (162 MHz, CD₂Cl₂, 25 °C): δ = 35.7^a (s); 33.3^b (s); ¹H NMR (400 MHz, CD₂Cl₂, 25 °C) δ = 7.44–7.85^{a,b} (m, 124.5H, CH_{Ph}), 7.10^a (s, 6.3H, CH_{Im}), 6.94^b (s, 2H, CH_{Im}), 4.15–4.25^a (m, 12.6H, NCH₂), 3.89–3.95^b (m, 2H, NCH₂), 3.62–3.69^b (m, 2H, NCH₂), 3.40–3.46^b (m, 2H, PCH), 3.15–3.22^a (m, 6.3H, PCH), 2.63–2.71^b (m, 2H, CH₂), 2.46–2.52^a (m, 6.3H, CH₂), 2.18–2.27^a (m, 6.3H, CH₂), 1.55–1.65^b (m, 2H, CH₂); ¹³C{¹H} NMR (100.6 MHz, CD₂Cl₂, 25 °C) δ = 183.2^a (t, J_{CP} = 5.0 Hz, CO), 181.4^b (brs, CO), 165.4^b (s, N₂C), 161.4^a (s, N₂C), 134.6^a (d, J_{CP} = 3.0 Hz, CH_{Ph}), 134.4^b (d, J_{CP} = 3.0 Hz, CH_{Ph}), 134.1^b (d, J_{CP} = 9.0 Hz, CH_{Ph}), 133.9^a (d, J_{CP} = 9.0 Hz, CH_{Ph}), 130.6^a (d, J_{CP} = 11.1 Hz, CH_{Ph}), 130.3^b (d, J_{CP} = 12.1 Hz, CH_{Ph}), 122.9^b (d, J_{CP} = 83.7 Hz, C_{Ph}), 122.8^a (s, CH_{Im}), 122.6^a (d, J_{CP} = 83.5 Hz, C_{Ph}), 121.8^b (s, CH_{Im}), 121.5^{a,b} (q, J_{CF} = 320.9 Hz, CF₃), 52.3^b (d, J_{CP}

= 16.1 Hz, NCH₂), 51.4^a (d, J_{CP} = 15.1 Hz, NCH₂), 26.3^b (s, CH₂), 25.4^a (s, CH₂), 11.5^b (d, J_{CP} = 35.2 Hz, PCH), 9.9^a (d, J_{CP} = 35.2 Hz, PCH). MS (ES⁺): m/z : 927.1 [M – (CF₃SO₃ + CO)]⁺; HRMS (ES⁺): calcd for C₄₆H₄₂F₃N₂O₃P₂PdS, 927.1394; found, 927.1411.

Single-crystal X-ray diffraction analyses of [2](Br), [3](OTf)₃, [4](OTf)₂, [5](OTf)₂, *meso*-[9](OTf)₂, and *dl*-[9](OTf)₂

Intensity data were collected at low temperature on an Apex2 Bruker diffractometer equipped with a 30W air-cooled microfocus source (λ = 0.71073 Å). The structures were solved using SUPERFLIP³⁷ or SIR92,³⁸ and refined by means of least-squares procedures using the programs of the PC version of CRYSTALS³⁹ or WINGX.⁴⁰ Atomic scattering factors were taken from the international tables for X-ray crystallography. All non-hydrogen atoms were refined anisotropically. For complex *dl*-[9](OTf)₂, a disorder found for a triflate anion has been refined as two partial-occupancy (0.6/0.4) triflate anions and a partial-occupancy (0.6) water molecule (oxygen O9). Moreover, two phenyl rings were disordered. The H atoms were located in a difference map, but those attached to carbon atoms were repositioned geometrically. The H atoms were initially refined with soft restraints on the bond lengths and angles to regularize their geometry (C-H in the range 0.93-0.98 Å, and $U_{iso}(H)$ in the range 1.2-1.5 times U_{eq} of the parent atom), after which the positions were refined with riding constraints. Absorption corrections were introduced using the program MULTISCAN.⁴¹

Supporting Information

The supporting Information of this article can be found under <https://...>

- NMR spectra for all new compounds (**2-10**),
- Crystallographic table for [2](Br), [3](OTf)₃, [4](OTf)₂, [5](OTf)₂, *meso*-[9](OTf)₂, and *dl*-[9](OTf)₂.
- Computational details and optimized structures of cationic Pd complexes **7**⁺, **8**²⁺, and **8**'²⁺.

Author Information

Corresponding author: *E-mail for Y.C.: yves.canac@lcc-toulouse.fr

ORCID

Yves Canac: 0000-0002-3747-554X

Noël Lugan: 0000-0002-3744-5252

Christine Lepetit: 0000-0002-0008-9506

Dmitry A. Valyaev: 0000-0002-1772-844X

Notes

The authors declare no competing financial interests.

Acknowledgements

The authors thank the Centre National de la Recherche Scientifique for financial support. Computational studies were performed using HPC resources from CALMIP (Grant 2018 [0851]) and from GENCI-[CINES/IDRIS] (Grant 2018 [085008]).

Notes and references

- 1 (a) D. Morales-Morales, C. G. M. Jensen, *The Chemistry of Pincer Compounds*, Elsevier Science: 2011; (b) G. Van Koten, D. Milstein, *Organometallic Pincer Chemistry*, ed. G. van Koten and D. Milstein, *Top. Organomet. Chem.*, 2013, **40**, 1–356; Springer-Verlag Berlin Heidelberg; (c) G. M. Adams, A. S. Weller, *Coord. Chem. Rev.* 2018, **355**, 150–172.
- 2 (a) G. van Koten, *Pure Appl. Chem.*, 1989, **61**, 1681–1694; (b) D. Benito-Garagorri, K. Kirchner, *Acc. Chem. Res.*, 2008, **41**, 201–203; (c) D. M. Roddick, D. Zargarian, *Inorg. Chim. Acta*, 2014, **422**, 251–264.
- 3 (a) Pincer and pincer-type complexes: applications in organic synthesis and catalysis, ed. K. J. Szabó, O. F. Wendt, Wiley-VCH, Weinheim, Germany, 2014; (b) G. Gunanathan, D. Milstein, *Chem. Rev.*, 2014, **114**, 12024–12087; (c) L. Maser, L. Vondung, R. Langer, *Polyhedron*, 2018, **143**, 28–42.
- 4 C. J. Moulton, B. L. Shaw, *J. Chem. Soc., Dalton Trans.*, 1976, 1020–1024.
- 5 M. L. H. Green, *J. Organomet. Chem.*, 1995, **500**, 127–148.
- 6 E. Peris, R. H. Crabtree, *Chem. Soc. Rev.*, 2018, **27**, 1959–1968.
- 7 LX₂-type pincer ligands whose the two anionic coordinating ends are in the central and peripheral position have already been reported, see for example: L. Luconi, A. Rossin, A. Motta, G. Tuci, G. Giambastiani, *Chem. Eur. J.*, 2013, **19**, 4906–4921.
- 8 (a) T. Agapie, M. W. Day, J. E. Bercaw, *Organometallics*, 2008, **27**, 6123–6142; (b) M. S. Winston, J. E. Bercaw, *Organometallics*, 2010, **29**, 6408–6416; (c) T. N. Lenton, D. G. VanderVelde, J. E. Bercaw, *Organometallics*, 2012, **31**, 7492–7499; (d) M. J. Islam, M. D. Smith, D. V. Peryshkov, *J. Organomet. Chem.*, 2018, **867**, 208–2013.
- 9 (a) E. Despagnet-Ayoub, L. M. Henling, J. A. Labinger, J. E. Bercaw, *Organometallics*, 2013, **32**, 2934–2938; (b) E. Borré, G. Dahm, A. Aliprandi, M. Mauro, S. Dagherne, S. Bellemin-Laponnaz, *Organometallics*, 2014, **33**, 4374–4384; (c) C Romain, C. Fliedel, S. Bellemin-Laponnaz, S. Dagherne, *Organometallics*, 2014, **33**, 5730–5739; (d) E. Despagnet-

-
- Ayoub, M. K. Takase, J. A. Labinger, J. E. Bercaw, *J. Am. Chem. Soc.*, 2015, **137**, 10500–10503; (e) D. Zhang, G. Zi, *Chem. Soc. Rev.*, 2015, **44**, 1898–1921.
- 10 (a) K. Kubo, N. D. Jones, M. J. Ferguson, R. McDonald, R. G. Cavell, *J. Am. Chem. Soc.*, 2005, **127**, 5314–5315; (b) W. Petz, B. Neumüller, *Polyhedron*, 2011, **30**, 1779–1784; (c) K. Kubo, H. Okitsu, H. Miwa, S. Kume, R. G. Cavell, *Organometallics*, 2017, **36**, 266–274.
- 11 Y. Canac, *Chem. Asian J.*, 2018, **13**, 1872–1887.
- 12 I. Benaissa, R. Taakili, N. Lugan, Y. Canac, *Dalton Trans.*, 2017, **46**, 12293–12305.
- 13 C. Barthes, C. Bijani, N. Lugan, Y. Canac, *Organometallics*, 2018, **37**, 673–678.
- 14 For NHC ligands, see: (a) D. Bourissou, O. Guerret, F. P. Gabbaï, G. Bertrand, *Chem. Rev.*, 2000, **100**, 39–91; (b) F. E. Hahn, M. C. Jahnke, *Angew. Chem. Int. Ed.*, 2008, **47**, 3122–3172; (c) D. J. Nelson, S. P. Nolan, *Chem. Soc. Rev.*, 2013, **42**, 6723–6753; (d) M. N. Hopkinson, C. Richter, M. Schedler, F. Glorius, *Nature*, 2014, **510**, 485–496. For phosphonium ylide ligands, see: (a) H. Schmidbaur, *Angew. Chem. Int. Ed. Engl.*, 1983, **22**, 907–927; (b) W. C. Kaska, K. A. Ostoja Starzewski, in: *Ylides and Imines of Phosphorus*; A. W. Johnson, Eds, John Wiley & Sons: New York, 1993, chapt. 14; (c) O. I. Kolodiaznyi, *Tetrahedron*, 1996, **52**, 1855–1929; (d) J. Vicente, M. T. Chicote, *Coord. Chem. Rev.*, 1999, **193–195**, 1143–1161; (e) E. P. Urriolabeitia, *Top. Organomet. Chem.*, R. Chauvin, Y. Canac, Eds, Springer, 2010, **30**, 15–48; (f) Y. Canac, R. Chauvin, *Eur. J. Inorg. Chem.*, 2010, 2325–2335.
- 15 For the unique precedent of a P-metalla-substituted phosphonium ylide pincer complex, see: Y. Nakajima, F. Ozawa, *Organometallics*, 2012, **31**, 2009–2015.
- 16 (a) L. R. Falvello, S. Fernández, R. Navarro, A. Rueda, E. P. Urriolabeitia, *Inorg. Chem.*, 1998, **37**, 6007–6013; (b) A. Spannenberg, W. Baumann, U. Rosenthal, *Organometallics*, 2000, **19**, 3991–3993; (c) E. Serrano, C. Vallés, J. J. Carbó, A. Lledós, T. Soler, R. Navarro, E. P. Urriolabeitia, *Organometallics*, 2006, **25**, 4653–4664; (d) E. Serrano, T. Soler, E. P. Urriolabeitia, *Eur. J. Inorg. Chem.*, 2013, 2129–2138; (e) E. Serrano, T. Soler, E. P. Urriolabeitia, *Eur. J. Inorg. Chem.*, 2017, 2220–2230.
- 17 A general classification of phosphonium bis-ylides has been proposed, see: M. Abdalilah, Y. Canac, C. Lepetit, R. Chauvin, *C. R. Chim.*, 2010, **13**, 1091–1098.
- 18 Attempts to convert imidazole **1** to bis(N-phosphonio) imidazolium salt [**3**]Br₃ in a one-pot manner using the following conditions (imidazole **1** (1.0 eq.), (3-bromopropyl)triphenylphosphonium bromide (2.2 eq), K₂CO₃ (3.0 eq.), DMF, molecular sieves, 120°C) only resulted in the formation of a mixture of unidentified products.

19 S. O. Grim, E. F. Davidoff, T. J. Marks, *Z. Naturforsch., B: Anorg. Chem. Org. Chem. Biochem. Biophys. Biol.*, 1971, **26**, 184–190.

20 CCDC 1865718 [2]Br, CCDC 1865721 [3](OTf)₃, CCDC 1865720 [4](OTf)₂, CCDC 1865719 [5](OTf)₂, and CCDC 1865716 *meso*-[9](OTf)₂, and CCDC 1865717 *dl*-[9](OTf)₂ contain the supplementary crystallographic data for this paper. These data can be obtained free of charge from the Cambridge Crystallographic Data Centre via www.ccdc.cam.ac.uk/data_request/cif.

21 Imidazolium and phosphonium derivatives are generally characterized by pK_a values between 20 and 24 in DMSO. For pK_a values, see: http://evans.rc.fas.harvard.edu/pdf/evans_pka_table.pdf.

22 C. J. O'Brien, E. A. B. Kantchev, C. Valente, N. Hadei, G. A. Chass, A. Lough, A. C. Hopkinson, M. G. Organ, *Chem. Eur. J.*, 2006, **12**, 4743–4748.

23 (a) Y. Canac, C. Duhayon, R. Chauvin, *Angew. Chem. Int. Ed.*, 2007, **46**, 6313–6315; (b) I. Abdellah, N. Debono, Y. Canac, C. Duhayon, R. Chauvin, *Dalton Trans.*, 2009, 7196–7202.

24 The addition of an equivalent of base results in a partial conversion of the PdCl₂ precursor [5](OTf)₂ and the formation of products whose ³¹P NMR resonances are in the classical range of Pd–ylide species.

25 The cyclopalladation of phosphonium ylides is a well-known process, especially in the case of stabilized ylides where selectivity issues have been carefully addressed, for relevant examples see: (a) L. R. Falvello, S. Fernández, R. Navarro, A. Rueda, E. P. Urriolabeitia, *Organometallics*, 1998, **17**, 5887–5900; (b) D. Aguilar, M. A. Aragüés, R. Bielsa, E. Serrano, R. Navarro, E. P. Urriolabeitia, *Organometallics*, 2007, **26**, 3541–3551.

26 Electrochemical measurements (10⁻³ M in CH₃CN, (nBu₄N)(OTf), Pt) indicated that the orthometallated Pd complex [7](OTf) (E_{ox} = +1.21 V vs. SCE) is oxidized more easily than the pincer Pd complex [8](OTf)₂ (E_{ox} = +2.00 V vs. SCE).

27 The coordinated CH₃CN molecule evidenced both by X-ray diffraction analysis and NMR spectroscopy in the Pd complex [8](OTf)₂ was not observed by spectroscopy IR either in a concentrated CH₂Cl₂ solution or in the solid state.

28 The calculation level was validated by the reasonable agreement between the optimized geometry and the available X-ray crystal structure of Pd complex [9](OTf)₂.

29 (a) J. G. P. Delis, P. G. Aubel, K. Vrieze, P. W. N. M. van Leeuwen, *Organometallics*, 1997, **16**, 2948–2957; (b) A. C. Badaj, G. G. Lavoie, *Organometallics*, 2013, **32**, 4577–4590.

30 The IR ν_{CN} frequency of free *t*-BuNC is observed at 2139 cm⁻¹ in CH₂Cl₂.

-
- 31 (a) P. Veya, C. Floriani, A. Chiesi-Villa, C. Rizzoli, *Organometallics*, 1994, **13**, 441–450;
(b) L. Canovese, F. Visentin, C. Levi, A. Dolmella, *Dalton Trans.*, 2011, **40**, 966–981.
- 32 (a) J. L. Bolliger, O. Blacque, C. M. Frech, *Angew. Chem. Int. Ed.*, 2007, **46**, 6514–6517;
(b) J. Lisena, J. Monot, S. Mallet-Ladeira, B. Martin-Vaca, D. Bourissou, *Organometallics*, 2013, **32**, 4301–4305.
- 33 C. A. Tolman, *J. Am. Chem. Soc.*, 1970, **92**, 2953–2956.
- 34 A. R. Chianese, X. Li, M. C. Janzen, J. W. Faller, R. H. Crabtree, *Organometallics*, 2003, **22**, 1663–1667.
- 35 E. P. Kündig, D. McIntosh, M. Moskovits, G. A. Ozin, *J. Am. Chem. Soc.*, 1973, **95**, 7234–7241.
- 36 (a) Y. Canac, C. Lepetit, M. Abdalilah, C. Duhayon, R. Chauvin, *J. Am. Chem. Soc.*, 2008, **130**, 8406–8413; (b) Y. Canac, C. Lepetit, *Inorg. Chem.*, 2017, **56**, 667–675.
- 37 L. Palatinus, G. Chapuis, *J. Appl. Cryst.*, 2007, **40**, 786–790.
- 38 A. Altomare, G. Cascarano, C. Giacovazzo, A. Guagliardi, M. C. Burla, G. Polidori, M. Camalli, *J. Appl. Cryst.*, 1994, **27**, 435–436.
- 39 P. W. Betteridge, J. R. Carruthers, R. I. Cooper, K. Prout, D. J. Watkin, *J. Appl. Cryst.*, 2003, **36**, 1487.
- 40 L. J. Farrugia, *J. Appl. Cryst.*, 2012, **45**, 849–854.
- 41 R. H. Blessing, *Acta Crystallogr.*, 1995, **A51**, 33–38.